WATER RESOURCES RESEARCH, VOL. 49, 565–584, doi:10.1029/2012WR012638, 2013

Optimizing environmental flows for multiple reaches affected by a multipurpose reservoir system in Taiwan: Restoring natural flow regimes at multiple temporal scales

Jenq-Tzong Shiau[1] and Fu-Chun Wu[2]

Received 6 July 2012; revised 1 December 2012; accepted 3 December 2012; published 30 January 2013.

[1] For reservoirs that are operated for multiple purposes such as water supply, flood control, and power generation, any attempts to incorporate environmental flow targets in the reservoir operation rules need to take into account both the human and ecosystem demands. To date, however, none of the reservoir operation schemes that consider environmental flow requirements includes subdaily flow regimes and is able to optimize for multiple reaches. Here, we address the temporal and spatial issues associated with the optimal environmental flow and operation strategies for a multipurpose reservoir system in Taiwan. We propose an environmental flow proportion strategy and three-period release approach, and multireach operation scenarios that simultaneously optimize reservoir performances and environmental flow objectives at subdaily to interannual timescales for a maximum of three connected reaches. Our results imply that taking into account the environmental flow objectives does not necessarily degrade the overall reservoir performance due to the positive effect on flood control, which in turn would compensate for the adverse effects on domestic water supply and hydropower generation. The three-period release approach benefits mainly the subdaily flow regime, while the environmental flow proportion strategy benefits primarily the daily flow regime. Spatially, a mutual exclusion is observed between the reaches above and below a diversion weir, a fact that revises the conventional perception that restoring the flow regimes of a downstream reach would automatically restore those of upstream reaches. An overall evaluation reveals that the three-reach scenario outperforms the two-reach scenarios, which then outperform the one-reach scenarios. The one- or two-reach scenario that incorporates the midstream reach may be taken as an alternative because such scenario would benefit the upstream or downstream reach in addition to the midstream reach.

Citation: Shiau, J.-T., and F.-C. Wu (2013), Optimizing environmental flows for multiple reaches affected by a multipurpose reservoir system in Taiwan: Restoring natural flow regimes at multiple temporal scales, *Water Resour. Res.*, *49*, doi:10.1029/2012WR012638.

1. Introduction

[2] The importance of "natural flow regime" (i.e., the natural flow variability in terms of magnitude, frequency, duration, timing, and rate of change) in sustaining river environments and aquatic ecosystems is well recognized among river scientists, stream ecologists, and water resources managers [*Poff et al.*, 1997; *Richter et al.*, 1997; *Whiting*, 2002; *Naiman et al.*, 2002; *Arthington et al.*, 2006; *Petts et al.*, 2006]. The natural flow regime has been increasingly adopted as a paradigm for river conservation and restoration. Motivated by this, over the last two decades, an enormous amount of research efforts have been devoted to the assessment of flow regime alterations caused by reservoir operation/flow regulation and/or determination of environmental flow patterns needed to restore (i.e., minimize the deviation from) the natural flow regime [e.g., *Richter et al.*, 1996, 1998; *Shiau and Wu*, 2004a, 2004b; *Batalla et al.*, 2004; *Harman and Stewardson*, 2005; *Magilligan and Nislow*, 2005; *Shiau and Wu*, 2006; *Suen and Eheart*, 2006; *Shiau and Wu*, 2007a, 2007b; *Mathews and Richter*, 2007; *Singer*, 2007; *Shiau and Wu*, 2008; *Hughes and Mallory*, 2008; *Shiau and Wu*, 2009; *Gao et al.*, 2009; *Shiau and Wu*, 2010; *Botter et al.*, 2010; *Reichold et al.*, 2010; *Yin et al.*, 2011]. The similarity among these studies is that they all compared the pre- and postimpact daily flow series to assess flow regime alterations at the intra-annual (e.g., daily, weekly, monthly, and seasonal) and interannual timescales; whereas different metrics, e.g., indicators of hydrologic alteration, histogram dissimilarity index, or probability density functions, were used in these studies to undertake the task of flow regime assessment or to evaluate the efficacies of the proposed environmental flow schemes on restoration of the interannual and intra-annual flow regimes.

[1]Department of Hydraulic and Ocean Engineering, National Cheng Kung University, Tainan, Taiwan.
[2]Department of Bioenvironmental Systems Engineering, Hydrotech Research Institute and Center for Ecological Engineering, National Taiwan University, Taipei, Taiwan.

Corresponding author: F.-C. Wu, Department of Bioenvironmental Systems Engineering, Hydrotech Research Institute and Center for Ecological Engineering, National Taiwan University, Taipei 106, Taiwan. (fcwu@ntu.edu.tw)

0043-1397/13/2012WR012638

[3] Recently, subdaily flow regimes started to gain more attention [*Zolezzi et al*., 2009; *Zimmerman et al*., 2010; *Meile et al*., 2011], owing to the adverse effects of severe subdaily flow regime alterations experienced, in particular, by those reaches where hydropower generation and dam operations caused drastic flow fluctuations within a 24 h period. It has been reported that this type of hydropeaking waves would disturb the stream substrate leading to catastrophic drift of benthic invertebrates [*Perry and Perry*, 1986; *Boon*, 1993; *Céréghino et al*., 2004; *Bruno et al*., 2010], strand juvenile fish in side channels or exposed areas due to rapid ramping, limit the nearshore shallow-margin habitat use and somatic growth rate [*Bradford*, 1997; *Saltveit et al*., 2001; *Scruton et al*., 2003; *Korman and Campana*, 2009], impact riparian biogeochemical processes such as hyporheic exchange, denitrification, and accumulation of biomass (algae and biofilms) [*Biggs and Close*, 1989; *Pinay et al*., 1995; *Battin et al*., 2003; *Breil et al*., 2007; *Sawyer et al*., 2009], thus would reduce the abundance, diversity, reproductive success, and survival of aquatic and riparian species [*Cushman*, 1985; *Blinn et al*., 1995; *Freeman et al*., 2001; *van Looy et al*., 2007; *Paetzold et al*., 2008]. Growing concerns for ecosystem conservation in recent years have led to the emergence of several mitigation measures, exemplified by the *Green Hydro* assessment procedure (a high ecological standard certification procedure for ecolabeling hydropower schemes, used in Switzerland) and multiscale environmental flow management (a suite of methodologies for environmental flow assessment across a spectrum of temporal and spatial scales, applied in Norway and Sweden) [*Bratrich et al*., 2004; *Halleraker et al*., 2007; *Renöfält et al*., 2010]. These approaches highlight the importance of mitigating the temporal and spatial impacts of hydropower generation in the context of multidisciplinary (hydrologic, geomorphologic, and ecological) considerations.

[4] The spatial extent of flow regime alterations is ecologically relevant since "hydrologic connectivity" is essential to the integrity of riverine ecosystems [*Pringle*, 2001]; the spatially cumulative effect of dams has been reported to homogenize regional flow regimes, creating conditions unfavorable for sustaining native biodiversity [*Poff et al*., 2007]. Such spatial issues have been addressed by several researchers. For instance, *Richter et al*. [1998] performed a spatial assessment of hydrologic alterations for multiple reaches affected by a series of reservoirs. *Zimmerman et al*. [2010] assessed the spatial effects of multiple dams that caused subdaily flow fluctuations. *Renöfält et al*. [2010] identified three types of river reaches impacted by hydropower generation and stressed the need to prioritize restoration efforts among multiple sites.

[5] For many reservoirs operated for multiple purposes such as water supply, flood control, and hydropower production, any attempts to incorporate environmental flow targets in the reservoir operation rules need to take into account both the human and ecosystem demands [*Richter and Thomas*, 2007]. Optimization algorithms have been widely used as a means to determine the optimal reservoir operation rules or optimal tradeoffs between environmental flow and human needs objectives [e.g., *Homa et al*., 2005; *Suen and Eheart*, 2006; *Shiau and Wu*, 2007b; *Hughes and Mallory*, 2008; *Dittmann et al*., 2009; *Shiau and Wu*, 2010; *Yin et al*., 2011]. These studies mainly relied on at-a-site daily flow series (or flow duration curves) and scenario simulations to determine the optimal environmental flow schemes and reservoir operation rules aiming to secure human demands while maintaining the interannual and intra-annual flow regimes. However, none of the previous reservoir operation schemes that consider environmental flow requirements includes subdaily flow regimes and is able to optimize for multiple reaches that are subjected to different classes of hydrologic impacts caused by multipurpose reservoir operations.

[6] In the present study, we address the temporal and spatial issues associated with optimal environmental flow and operation strategies for a multipurpose reservoir system in Taiwan. We present a novel environmental flow proportion strategy, a three-period release approach, and multireach operation scenarios that simultaneously optimize reservoir performances and environmental flow objectives at five temporal scales (subdaily to interannual scales) for a maximum of three connected reaches. This paper is organized as follows. In section 2, an overview of the Feitsui Reservoir system and current operation rules is given. In section 3, the proposed environmental flow and reservoir release strategies are described. In section 4, the integrated simulation-optimization framework and multireach operation scenarios are summarized. In section 5, the results are presented and discussed. The conclusions and implications of this study are provided in section 6.

2. Feitsui Reservoir System

2.1. Overview

[7] The Feitsui Reservoir dams the Peishih Creek (north fork of the upper Hsintien Creek) located in northern Taiwan (Figure 1). This multipurpose facility (with an active capacity of 335.5×10^6 m^3 and maximum surface area and depth of 10.24 km^2 and 113.5 m, respectively) has been in operation since 1987 to supply the domestic water demand of the Taipei metropolitan area [*Taipei Feitsui Reservoir Administration* (*TFRA*), 2004]. The associated run-of-river power plant (with a capacity of 70 MW) facilitates peaking hydropower generation. The reservoir also serves to attenuate flood peaks during typhoons. The domestic water demands (Table 1) are jointly supplied by the reservoir and Nanshih Creek (south fork of the upper Hsintien Creek). The merged flow is diverted from the Chingtan Weir to the water treatment plant and then distributed to domestic users by the Taipei Water Company (Figure 2).

[8] Spatially, the three connected reaches of the system are subjected to different classes of hydrologic impact. Reach A, located immediately below the reservoir, is directly affected by reservoir operations and categorized as a "regulated but unimpounded" reach according to *Renöfält et al*. [2010]. Reach B, located below a confluence merging the regulated flow (from Reach A) and unregulated flow (from Nanshih Creek), is subjected to the run-of-river impoundment effect of the Chingtan Weir and categorized as a reach "with reservoirs and impoundments" [*Renöfält et al*., 2010]. Reach C, located downstream of the Chingtan Weir, is subjected to the cumulative effects of reservoir operations, unregulated tributary inflows and flow diversions, is categorized as a reach "with

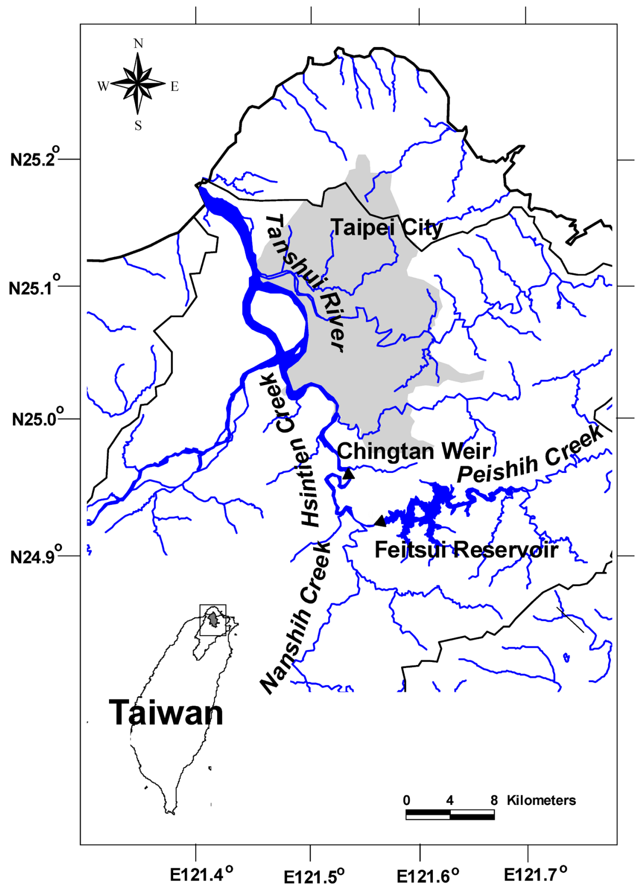

Figure 1. Location map of Feitsui Reservoir system. The Feitsui Reservoir dams the Peishih creek (north fork of upper Hsintien Creek). The merged flow from the Feitsui Reservoir and Nanshih Creek (south fork of upper Hsintien Creek) is diverted from the Chingtan Weir to supply the domestic water demands of the Taipei metropolitan area.

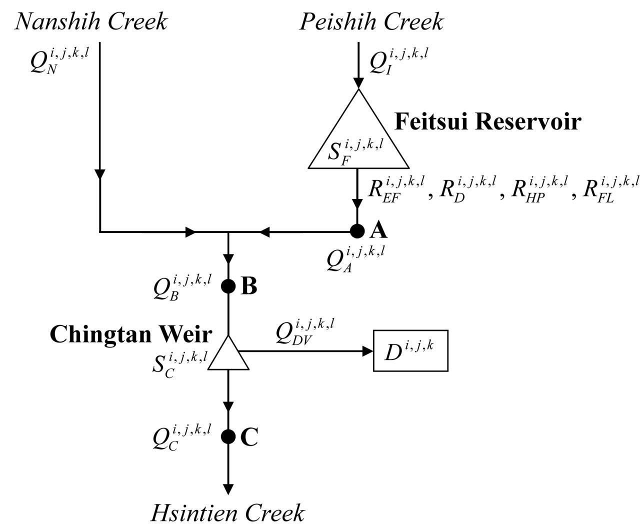

Figure 2. Flow diagram and facilities of Feitsui Reservoir system. See text for notations.

reduced discharge" [*Renöfält et al*., 2010]. These spatially different hydrologic alterations will be taken into account as we seek to optimize environmental flow schemes and reservoir operation rules to restore the natural flow regimes at the three reaches.

[9] The inflows of the Feitsui Reservoir are collected by the TFRA, while the flows of the Nanshih Creek are collected by the Taiwan Power Company (TPC). Hourly incoming flows are recorded during the flood periods, whereas only three data per day (at 0:00 A.M., 8:00 A.M., and 4:00 P.M.) are recorded during the nonflood periods. The flow series (1998–2008) used in this study were provided by the TFRA and TPC. Some monthly means are shown in Table 1, which include the mean reservoir inflows, mean flows of the Nanshih Creek, and converted mean flows for the projected domestic demands. The annual reservoir inflow is ~1.1 billion m^3 (daily inflow = 34.2 m^3/s), while the annual runoff of the Nanshih Creek is ~1.3 billion m^3 (daily flow = 40.4 m^3/s). The annual domestic water demand is ~1.1 billion m^3 (daily diversion = 35.8 m^3/s). Table 1 reveals that, during the dry months, the incoming flows from the Nanshih Creek alone are insufficient to fully supply the domestic water demands.

2.2. Current Operation Rules

[10] The multipurpose operations of the Feitsui Reservoir system are based on the hourly timescale. First, the domestic water demand is primarily supplied by the Nanshih Creek, with the water deficits supplemented by reservoir releases [*TFRA*, 2004]. The daily amount of water to be released for domestic water supply, $DR^{i,j,k}$, is determined at the first hour (0:00 A.M.) of each day based on the reservoir water level and incoming flow from the Nanshih Creek (see Appendix A1), where $DR^{i,j,k}$ total amount of water to be released on the *k*th day, *j*th month, *i*th year. This daily amount of water release is evenly distributed in 8 h from 8:00 A.M. to 4:00 P.M. (ninth to sixteenth hour), such that the hourly release rate can be determined by

Table 1. Monthly Mean Inflows of Feitsui Reservoir, Mean Flows from Nanshih Creek, Projected Daily Domestic Demands, Converted Mean Flows for Projected Domestic Demands, and Daily Mean Evaporation Rates

Item	Jan	Feb	Mar	Apr	May	Jun	Jul	Aug	Sep	Oct	Nov	Dec
Mean inflow of Feitsui Reservoir (m^3/s)	21.8	27.0	18.9	16.2	26.5	33.3	26.9	32.2	79.7	57.2	40.5	30.5
Mean flow from Nanshih creek (m^3/s)	21.1	25.3	20.9	17.3	26.4	33.4	38.9	54.4	95.0	71.0	46.4	34.0
Projected daily domestic demand (10^6 m^3/d)	3.01	3.02	3.03	3.05	3.05	3.23	3.22	3.20	3.19	3.02	3.03	3.04
Mean flow for projected domestic demand (m^3/s)	34.9	34.9	35.1	35.3	35.4	37.4	37.3	37.1	37.0	35.0	35.1	35.2
Daily mean evaporation rate (mm/d)	1.05	1.30	1.85	2.72	3.03	3.21	4.67	4.62	3.46	2.16	1.33	1.04

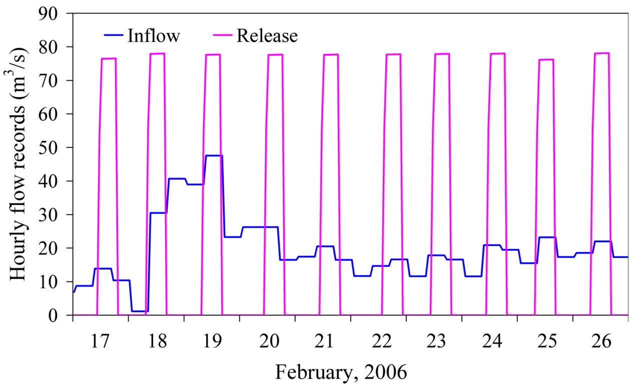

Figure 3. Inflows and releases of Feitsui Reservoir (17–26 February 2006). It is evident that the preimpact subdaily flow regime (pattern of inflows) is replaced by the hydropeaking waves (periodic releases and closures).

$$R_D^{i,j,k,l} = \begin{cases} \dfrac{\mathrm{DR}^{\,i,j,k}}{8\Delta t} & \text{for } 9 \le l \le 16 \\ 0 & \text{for } l < 9 \text{ or } l > 16 \end{cases}, \tag{1}$$

where $R_D^{i,j,k,l}$ = hourly release rate (for domestic water supply) at the lth hour, kth day, jth month, and ith year; Δt = operational time interval (= 1 h = 3600 s).

[11] Second, the release flow rate/duration for hydropower generation is also determined at 0:00 A.M. each day based on the reservoir storage [*TFRA*, 2004]. If the reservoir water level is between the upper and middle rule curves, the release of $R_{\mathrm{HP}}^{i,j,k,l}$ lasted for 8 h (8:00 A.M. to 4:00 P.M.) for peaking hydropower generation (see Appendix A2), where $R_{\mathrm{HP}}^{i,j,k,l}$ = hourly release rate (for hydropower generation) at the lth hour, kth day, jth month, and ith year. If the reservoir water level is above the upper rule curve, the release of $R_{\mathrm{HP}}^{i,j,k,l}$ lasts for 24 h. No flow would be released for hydropower generation if the reservoir water level is below the middle rule curve.

[12] Third, a three-stage compelling release for flood control is implemented during the typhoon period based on the hourly reservoir inflows and water levels $Q_I^{i,j,k,l}$ and $\mathrm{EL}_F^{\,i,j,k,l}$ [*TFRA*, 2004]. The first stage is the antecedent flood stage, in which the hourly release rate $R_{\mathrm{FL}}^{i,j,k,l}$ (for flood control) is targeted at reserving the spare capacity for flood detention. The second is the prepeak stage, where the release of $R_{\mathrm{FL}}^{i,j,k,l}$ is aimed to attenuate flood peaks and secure dam safety. The third is the postpeak stage, where the release of $R_{\mathrm{FL}}^{i,j,k,l}$ is to resume normal water levels and secure water storage available for post-flood supplies (for details, see Appendix A3). It should be noted here that such operation rules are typical of other multipurpose reservoir systems in Taiwan. For example, the Shihmen Reservoir uses similar operation rules (but different parameters) to provide irrigation and domestic water supplies, power generation, and flood control for the Taoyuan area (northern Taiwan) [*Suen and Eheart*, 2006].

[13] The flow releases for the domestic water supply pass through the power plant and will be used for peaking hydropower generation. The compelling flow release for flood control, however, is an emergency large flow release (>1000 m^3/s) through separate spillways, thus will not pass through the power plant (whose maximum allowable discharge = ~100 m^3/s). As such, the hourly total release rate from the reservoir is determined by

$$R_T^{i,j,k,l} = \max\left\{R_D^{i,j,k,l}, R_{\mathrm{HP}}^{i,j,k,l}\right\} + R_{\mathrm{FL}}^{i,j,k,l}. \tag{2}$$

[14] Figure 3 shows the hourly inflows and release rates of the reservoir during 17–26 February 2006. It is clear that, downstream of the reservoir, the natural subdaily flow regime (pattern of inflows) is replaced by the hydropeaking waves (periodic releases and closures). Finally, the hourly diversion rate at the Chingtan Weir (for domestic water supply), $Q_{\mathrm{DV}}^{i,j,k,l}$, is determined by

$$Q_{\mathrm{DV}}^{i,j,k,l} = \begin{cases} R_D^{i,j,k,l} + Q_N^{i,j,k,1}, & \text{if } \mathrm{DR}^{\,i,j,k} > 0 \\ \dfrac{D^{i,j,k}}{24\Delta t}, & \text{if } \mathrm{DR}^{\,i,j,k} = 0 \end{cases} \tag{3}$$

where $Q_N^{i,j,k,1}$ = flow from the Nanshih Creek at the first hour of each day; $D^{i,j,k}$ = projected daily domestic demand (Table 1).

3. Proposed Environmental Flow and Reservoir Release Strategies

3.1. Environmental Flow Proportion Strategy

[15] We propose an environmental flow strategy to preserve specified proportions of the incoming flows from the Nanshih and Peishih Creeks as the environmental flows, denoted as $\lambda_1 Q_N^{i,j,k,l}$ and $\lambda_2 Q_I^{i,j,k,l}$, where λ_1 and λ_2 are specified environmental flow proportions for the Nanshih and Peishih Creeks, respectively. The idea behind this strategy is to mimic the temporal pattern of the natural flow regime, even though the mean discharge is inevitably reduced. The environmental flow proportion λ_1 of the Nanshih Creek can be controlled by the flow diversions from the Chingtan Weir, while the environmental flow proportion λ_2 of the Peishih Creek is controlled by the flow releases from the Feitsui Reservoir (Figure 2); both are decision variables to be optimized in this study (see section 4.2).

[16] The hourly releases of environmental flow from the reservoir, $R_{\mathrm{EF}}^{i,j,k,l}$, are implemented in conjunction with the compelling flow release (for flood control) and is determined at the first hour of each day based on the reservoir inflow $Q_I^{i,j,k,1}$, expressed as

$$R_{\mathrm{EF}}^{i,j,k,l} = \begin{cases} \lambda_2 Q_I^{i,j,k,1}, & \text{if } Q_I^{i,j,k,1} < T_I \\ \begin{cases} \lambda_2 Q_I^{i,j,k,1} - R_{\mathrm{FL}}^{i,j,k,l} & \text{for } R_{\mathrm{FL}}^{i,j,k,l} < \lambda_2 Q_I^{i,j,k,1} \\ 0 & \text{for } R_{\mathrm{FL}}^{i,j,k,l} \ge \lambda_2 Q_I^{i,j,k,1} \end{cases}, & \text{if } Q_I^{i,j,k,1} \ge T_I. \end{cases} \tag{4}$$

[17] Given that a specified proportion λ_1 of the incoming flow from the Nanshih Creek is now preserved as the environmental flow, the daily release for domestic water supply, $\mathrm{DR}^{i,j,k}$, which is given in (A1), should be modified as

$$\mathrm{DR}^{\,i,j,k} = \begin{cases} \min\left\{C_{\mathrm{RC}}\left[D^{i,j,k} - 24\Delta t(1-\lambda_1)Q_N^{i,j,k,1}\right],\ S_F^{i,j,k,1} + 24\Delta t\ \left(Q_I^{i,j,k,1} - R_{\mathrm{EF}}^{i,j,k,1}\right) - S_F^{\min}\right\}, \\ \qquad \text{if } 24\Delta t(1-\lambda_1)Q_N^{i,j,k,1} < D^{i,j,k} \\ 0, \qquad \text{if } 24\Delta t(1-\lambda_1)Q_N^{i,j,k,1} \geq D^{i,j,k} \end{cases}, \tag{5}$$

where the minimum criterion is to ensure that the total release is less than the reservoir storage, $S_F^{i,j,k,1}$ = reservoir storage at the first hour of each day; $S_F^{\min}$ = dead storage of the reservoir (= 48.7 million m^3); the release coefficient C_{RC} is determined by (A2), where the hedging coefficients $C_{\mathrm{RC}}^3, C_{\mathrm{RC}}^4, C_{\mathrm{RC}}^5$ now become decision variables to be optimized (see section 4.2).

3.2. Three-Period Release Approach

[18] To mitigate the hydropeaking effects, we propose a three-period release approach to redistribute the release amounts and periods for the domestic water supply and hydropower generation. As a first step, the release period for the domestic water supply is redistributed in 24 h that is divided into two subperiods (Figure 4), where a major fraction γ of the daily total amount $\mathrm{DR}^{i,j,k}$ is released in the first period d_1 while the rest is released in the second period $(24-d_1)$. The release rates in these two periods are expressed as

$$R_D^{i,j,k,l} = \begin{cases} \dfrac{\gamma \mathrm{DR}^{\,i,j,k}}{d_1\Delta t} & \text{for } l_1 \leq l \leq l_2 \\ \dfrac{(1-\gamma)\mathrm{DR}^{\,i,j,k}}{(24-d_1)\Delta t} & \text{for } l < l_1 \text{ or } l > l_2 \end{cases}, \tag{6}$$

where $(l_1,\ l_2)$ = starting and ending hours of d_1, respectively, with $0<d_1<24$. Here, to ensure that d_1 is distributed in the middle of the day (from the ninth to sixteenth hour), (l_1, l_2) are constrained by

$$l_1 = 10 - \left[\frac{d_1-6}{2}\right],\ l_2 = 9 - \left[\frac{d_1-6}{2}\right] + d_1, \tag{7}$$

where $[\cdot]$ = maximum integer<the argument. The release parameters d_1 and γ are decision variables to be optimized in this study (see section 4.2).

[19] As a second step, the releases for peaking hydropower generation are distributed in the third period d_2 (Figure 4), and the release rule given in (A3) is modified accordingly as

$$R_{\mathrm{HP}}^{i,j,k,l} = \begin{cases} Q_{\mathrm{DP}}(\mathrm{EL}_F^{\,i,j,k,1}) & \text{for 24 h, if } \mathrm{EL}_F^{\,i,j,k,1} \geq RC_1^{j,k} \\ \begin{cases} Q_{\mathrm{DP}}(\mathrm{EL}_F^{\,i,j,k,1}) & \text{for } l_3 \leq l \leq l_4 \\ 0 \ \text{ for } \ l < l_3 & \text{or } l > l_4 \end{cases}, \text{if } \mathrm{RC}_2^{j,k} \leq \mathrm{EL}_F^{\,i,j,k,1} < \mathrm{RC}_1^{j,k} \\ 0 \ \text{ for } \ 24 \text{ h}, \quad \text{if } \mathrm{EL}_F^{\,i,j,k,1} < \mathrm{RC}_2^{j,k} \end{cases}, \tag{8}$$

where Q_{DP} is design discharge for power generation (see Appendix A2 for details); $(l_3,\ l_4)$ = starting and ending hours of d_2, respectively, with $1\leq d_2 \leq 16$. Again, to ensure that d_2 is distributed in the middle of the day, $(l_3,\ l_4)$ are constrained by

$$l_3 = 11 - \left[\frac{d_2-4}{2}\right], \qquad l_4 = 10 - \left[\frac{d_2-4}{2}\right] + d_2. \tag{9}$$

The release parameter d_2 is also a decision variable to be optimized (see section 4.2).

[20] With the environmental flow strategy incorporated in the reservoir operation rule, the hourly total release rate from the reservoir is now modified as

$$R_T^{i,j,k,l} = \max\left\{R_{\mathrm{EF}}^{i,j,k,l} + R_D^{i,j,k,l}, \quad R_{\mathrm{HP}}^{i,j,k,l}\right\} + R_{\mathrm{FL}}^{i,j,k,l}, \tag{10}$$

where the environmental flow release rate $R_{\mathrm{EF}}^{i,j,k,l}$ is determined by (4), the release rate for the domestic water supply $R_D^{i,j,k,l}$ is determined by (6), the release rate for the hydropower generation $R_{\mathrm{HP}}^{i,j,k,l}$ is determined by (8), and the compelling release for flood control $R_{\mathrm{FL}}^{i,j,k,l}$ is determined by (A4), with the parameters T_I, α_1, α_2, α_3, α_4, α_5, α_6 being decision variables to be optimized in this study (see section 4.2). Again, since a specified proportion λ_1 of the flow from the Nanshih Creek is now reserved as the environmental flow, the diversion rate at the Chingtan Weir (for domestic water supply) is modified as

$$Q_{\mathrm{DV}}^{i,j,k,l} = \begin{cases} R_D^{i,j,k,l} + (1-\lambda_1)Q_N^{i,j,k,1}, \text{ if } \mathrm{DR}^{\,i,j,k} > 0 \\ \dfrac{D^{i,j,k}}{24\Delta t}, \qquad \text{if } \mathrm{DR}^{\,i,j,k} = 0 \end{cases}, \tag{11}$$

where the daily total release $\mathrm{DR}^{i,j,k}$ is determined by the modified criterion given in (5).

4. Simulation-Optimization Framework

[21] To simultaneously optimize reservoir performances and environmental flow objectives, we construct a simulation-optimization framework that uses a routing model to simulate the spatial distribution of flows in the three study

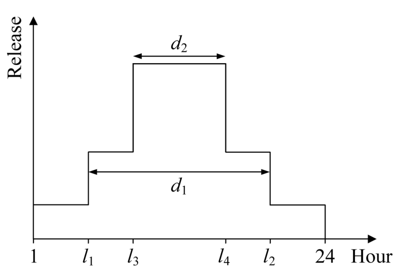

Figure 4. Three-period release approach to redistributing the release amounts and periods for domestic water supply and hydropower generation. The release period for the domestic water supply is redistributed in 24 h that is divided into two subperiods, where a major fraction γ of the daily amount $\mathrm{DR}^{i,j,k}$ is released in the first period d_1 while the rest is released in the second period $(24-d_1)$. The releases for the peaking hydropower generation are distributed in the third period d_2.

reaches under the specified set of parameter values (λ_1, λ_2, γ, d_1, d_2, C^3_{RC}, C^4_{RC}, C^5_{RC}, T_I, α_1, α_2, α_3, α_4, α_5, α_6), where the release rates from the Feitsui Reservoir and diversion rates at the Chingtan Weir are determined via (10) and (11). The routing model is integrated with a multiobjective optimization framework to solve for the optimal operational parameters, as described in the subsequent sections.

4.1. Simulation Model

[22] Routing of the flows at the three reaches of the system is based on the water continuity equation. The hourly discharge at Reach A, $Q_A^{i,j,k,l}$, is given by

$$Q_A^{i,j,k,l} = R_T^{i,j,k,l} + R_{\mathrm{SP}}^{i,j,k,l}, \tag{12}$$

where $R_{\mathrm{SP}}^{i,j,k,l}$ = hourly reservoir spill (see Appendix B1). The hourly discharge at Reach B, $Q_B^{i,j,k,l}$, is the sum of the incoming flows from Reach A and Nanshih Creek:

$$Q_B^{i,j,k,l} = Q_A^{i,j,k,l} + Q_N^{i,j,k,l}. \tag{13}$$

[23] The hourly flow at Reach C, $Q_C^{i,j,k,l}$, is the sum of the preserved environmental flows from the Peishih and Nanshih Creeks and flow spill from the Chingtan Weir (see Appendix B2).

4.2. Optimization Framework

4.2.1. Metrics for Reservoir Performance

[24] Five indices are used in this study to evaluate the multipurpose reservoir performances, including three for domestic water supply, one for hydropower generation, and one for flood control. These are described as follows:

1. *Indices for Domestic Water Supply*. To evaluate the reservoir performances in domestic water supply, first, we calculate the daily water shortage $\mathrm{DWS}^{\,i,j,k}$ as follows:

$$\mathrm{DWS}^{\,i,j,k} = \left| \min\left\{ \sum_{l=1}^{24} Q_{\mathrm{DV}}^{i,j,k,l} \Delta t - D^{i,j,k},\ 0 \right\} \right|. \tag{14}$$

[25] Three indices are then defined using the daily water shortages [*Shiau and Wu*, 2010]. The first one is the long-term total shortage ratio (TSR), defined as the ratio of total deficit to total demand over the study period, which is expressed as

$$\mathrm{TSR} = \frac{\sum_{i=1}^{N_Y}\sum_{j=1}^{12}\sum_{k=1}^{N_j} \mathrm{DWS}^{\,i,j,k}}{\sum_{i=1}^{N_Y}\sum_{j=1}^{12}\sum_{k=1}^{N_j} D^{i,j,k}} \times 100\%, \tag{15}$$

where N_Y = number of years in the study period; N_j = number of days in the *j*th month. The second index is the mean annual deficit duration (ADD), which is defined as

$$\mathrm{ADD} = \frac{1}{N_Y}\sum_{i=1}^{N_Y}\sum_{j=1}^{12}\sum_{k=1}^{N_j} \begin{cases} 1, & \text{if } \mathrm{DWS}^{\,i,j,k} > 0 \\ 0, & \text{if } \mathrm{DWS}^{\,i,j,k} = 0 \end{cases}. \tag{16}$$

The third index is the maximum 1 day shortage ratio (MSR), which is a measure indicating the extreme deficit condition and is defined by

$$\mathrm{MSR} = \max_{i,j,k} \left\{ \frac{\mathrm{DWS}^{\,i,j,k}}{D^{i,j,k}} \right\} \times 100\%. \tag{17}$$

2. *Index for Hydropower Generation*. The mean annual hydropower production (AHP) is used to evaluate the reservoir performance in hydropower generation, which is calculated as follows [*TFRA*, 2004]:

$$\mathrm{AHP} = \frac{1}{N_Y}\sum_{i=1}^{N_Y}\sum_{j=1}^{12}\sum_{k=1}^{N_j}\sum_{l=1}^{24} 9.8\eta H_E^{i,j,k,l} R_{\mathrm{HP}}^{i,j,k,l}, \tag{18}$$

where AHP is in kWh/yr; η is the efficiency of power generation (%); $H_E^{i,j,k,l}$ is the hourly effective head for power generation (m); given η and H_E varying as a function of the reservoir water level (see Appendix A2, Table 4).

3. *Index for Flood Control*. The maximum flood attenuation (MFA) is used to assess the reservoir performance in flood control, which is defined as the maximum difference between the reservoir inflow and outflow during the study period [*Shiau and Wu*, 2010] and is expressed as

$$\mathrm{MFA} = \max_{i,j,k,l} \left\{ Q_I^{i,j,k,l} - Q_A^{i,j,k,l} \right\}. \tag{19}$$

4.2.2. Metrics for Environmental Flow Performance

[26] In this study, the environmental flow release is aimed to minimize the deviation of the postimpact flow regimes from the preimpact ones at subdaily, daily, seasonal, annual, and interannual scales. Five hydrologic indices are used here to evaluate flow regime alterations at these timescales. For operation scenarios that consider multiple reaches, these indices are calculated for each individual reach, which are described as follows:

1. *Subdaily Index*. The Richards-Baker flashiness (RBF) index [*Baker et al.*, 2004] is used to assess the degree of subdaily flow oscillations. This index has been used to evaluate the effects of dams on subdaily flow regimes [*Zimmerman et al.*, 2010]. The RBF index is defined as the path length of flow oscillations (= sum of the absolute values of hour-to-hour changes in flow) divided by the sum of hourly flows over each 24 hour period. For Reach A, the RBF index of the natural flow regime is expressed as

$$\mathrm{RBF}_{\mathrm{NA}}^{\,i,j,k} = \frac{\sum_{l=2}^{24} |Q_I^{i,j,k,l} - Q_I^{i,j,k,l-1}|}{\sum_{l=1}^{24} Q_I^{i,j,k,l}}. \tag{20}$$

[27] The RBF index of the altered flow regime is expressed as

$$\mathrm{RBF}_{\mathrm{AA}}^{\,i,j,k} = \frac{\sum_{l=2}^{24} |Q_A^{i,j,k,l} - Q_A^{i,j,k,l-1}|}{\sum_{l=1}^{24} Q_A^{i,j,k,l}} \tag{21}$$

The mean difference between the natural and altered values of RBF, denoted as $\Delta\mathrm{RBF}_A$, is then used to quantify the degree of hydrologic alteration at subdaily timescale:

$$\triangle\text{RBF}_A = \frac{\sum_{i=1}^{N_Y}\sum_{j=1}^{12}\sum_{k=1}^{N_j}|\text{RBF}_{\text{NA}}^{i,j,k} - \text{RBF}_{\text{AA}}^{i,j,k}|}{\sum_{i=1}^{N_Y}\sum_{j=1}^{12}\sum_{k=1}^{N_j}1}. \tag{22}$$

The natural and altered values of RBF and the ΔRBF indices for Reaches B and C can be evaluated in a similar way, where the natural flows are the sum of $Q_I^{i,j,k,l}$ and $Q_N^{i,j,k,l}$.

2. *Daily Index*. The daily hydrographs are indicative of the daily-scale flow variations, as illustrated in Figure 3. To quantify the variability of the daily-scale flow pattern, here, we devise a daily hydrograph dissimilarity (DHD) index, which is defined as the mean daily difference between the day-to-day hydrographs of hourly flows divided by the mean daily flow over each 1 year period. For Reach A, the yearly DHD index of the natural flow regime (for the *i*th year), denoted as $\text{DHD}_{\text{NA}}^{i}$, is calculated by

$$\text{DHD}_{\text{NA}}^{i} = \frac{\frac{1}{365\times 364/2}\sum_{m=1}^{364}\sum_{n=m+1}^{365}\sum_{l=1}^{24}|Q_I^{i,m,l} - Q_I^{i,n,l}|}{\frac{1}{365}\sum_{m=1}^{365}\sum_{l=1}^{24}Q_I^{i,m,l}}, \tag{23}$$

where $Q_I^{i,m,l}$ is the reservoir inflow at the *l*th hour of the *m*th Julian day, *i*th year. The yearly DHD index of the altered flow regime is obtained by

$$\text{DHD}_{\text{AA}}^{i} = \frac{\frac{1}{365\times 364/2}\sum_{m=1}^{364}\sum_{n=m+1}^{365}\sum_{l=1}^{24}|Q_A^{i,m,l} - Q_A^{i,n,l}|}{\frac{1}{365}\sum_{m=1}^{365}\sum_{l=1}^{24}Q_A^{i,m,l}}. \tag{24}$$

[28] The mean difference between the natural and altered values of DHD over the study period, denoted as ΔDHD_A, is used to evaluate the daily-scale degree of hydrologic alteration:

$$\triangle\text{DHD}_A = \frac{1}{N_Y}\sum_{i=1}^{N_Y}|\text{DHD}_{\text{NA}}^{i} - \text{DHD}_{\text{AA}}^{i}|. \tag{25}$$

The natural and altered values of yearly DHD and the ΔDHD indices for Reaches B and C can be evaluated in a similar manner.

3. *Seasonal Index*. The monthly flow hydrograph is indicative of the seasonal wet/dry patterns. To assess the alteration of seasonal flow regime, the monthly flow deviation index (ΔMFH) is employed here [*Shiau and Wu*, 2010], which is defined as the mean annual total deviation of the postimpact monthly flows from their preimpact counterpart. For Reach A, the ΔMFH index is calculated as follows:

$$\triangle\text{MFH}_A = \frac{1}{N_Y}\sum_{i=1}^{N_Y}\sum_{j=1}^{12}|Q_I^{i,j} - Q_A^{i,j}|, \tag{26}$$

where $Q_I^{i,j}$ and $Q_A^{i,j}$ preimpact and postimpact monthly mean flows. The ΔMFH indices for Reaches B and C can be evaluated in a similar manner, where the preimpact monthly mean flows at these reaches are both $\left(Q_N^{i,j} + Q_I^{i,j}\right)$.

4. *Annual Index*. Low flows are, in general, regarded as ecologically relevant because they provide annual periods of high productivity [*Richter et al.*, 1996]. Here, we take the annual 7 day minimum flow as a measure of annual low-flow characteristics [*Shiau and Wu*, 2010]. The mean deviation of the postimpact annual low flows from their preimpact counterpart, denoted as ΔALF, is used to quantify the degree of hydrologic alteration at annual timescale. For Reach A, the ΔALF index is calculated as follows:

$$\triangle\text{ALF}_A = \frac{1}{N_Y}\sum_{i=1}^{N_Y}|\text{ALF}^{i}(Q_I) - \text{ALF}^{i}(Q_A)|, \tag{27}$$

where $\text{ALF}^{i}(\cdot)$ = annual 7 day minimum flow of the argument flow series (for the *i*th year). The ΔALF indices for Reaches B and C can be evaluated in a similar way.

5. *Interannual Index*. Large floods are environmentally crucial because they maintain the alluvial channel forms featuring suitable conditions for physical habitat [*Whiting*, 2002]. It has been also reported that floods with 5 year recurrence interval provide sufficient flows for preventing disconnection of riparian zones [*Magilligan et al.*, 2003]. Here, the 5 year flood is used as a measure representative of the interannual large floods [*Shiau and Wu*, 2010], where the 5 year floods are obtained by a frequency analysis on the annual 1 h maximum flows. The deviation of the postimpact 5 year flood from its preimpact counterpart, denoted as ΔFLD, is used to quantify the degree of hydrologic alteration at interannual timescale. For Reach A, the ΔFLD index is calculated as follows:

$$\triangle\text{FLD}_A = |\text{FLD}_5(Q_I) - \text{FLD}_5(Q_A)|, \tag{28}$$

where $\text{FLD}_5(\cdot)$ = 5 year flood derived from the argument flow series. The ΔFLD indices for Reaches B and C can be evaluated in a similar way. The preimpact 5 year flood is 3550 m^3/s at Reach A and 4940 m^3/s at Reaches B and C.

4.2.3. Multiobjective Optimization Approach

[29] Optimizing all the aforementioned indices constitutes a multiobjective optimization problem. The corresponding objective functions may be expressed as

$$\text{Minimize}\{\text{TSR, ADD, MSR}, \triangle\text{RBF}, \triangle\text{DHD}, \triangle\text{MFH}, \triangle\text{ALF}, \triangle\text{FLD}\} \text{ and Maximize}\{\text{AHP, MFA}\} \tag{29}$$

[30] Because each index spans a different range of values, we employ the following relation to normalize the value of each index [*Shiau and Wu*, 2010]:

$$\text{OBJ}_i' = \frac{\text{OBJ}_i - \min(\text{OBJ}_i)}{\max(\text{OBJ}_i) - \min(\text{OBJ}_i)}, \tag{30a}$$

$$\text{OBJ}_i' = \frac{\max(\text{OBJ}_i) - \text{OBJ}_i}{\max(\text{OBJ}_i) - \min(\text{OBJ}_i)}, \tag{30b}$$

in which OBJ_i and OBJ_i' = original and normalized values of the *i*th index (i = 1 to 20), respectively; max (OBJ_i) and min (OBJ_i) = maximum and minimum values of the *i*th index (Table 2), respectively. Equations (30a) and (30b) are used for the indices in (29) that are to be minimized and maximized, respectively, which ensure that the normalized indices are bounded by [0,1], where the most and least favorable values are 0 and 1, respectively. The objective

Table 2. Maximum and Minimum Values of Performance Evaluation Indices

Category		Index	Maximum[a]	Minimum[a]
Reservoir indices		TSR (%)	87.45	0.68
		ADD (d/yr)	365.27	22.91
		MSR (%)	100	15.35
		AHP (kWh/yr)	200.2	0
		MFA (m^3/s)	4074.9	2624.2
Reachwise environmental flow indices	Reach A	ΔRBF_A (1/d)	1.87	0.03
		ΔDHD_A (1/yr)	0.85	0.03
		ΔMFH_A (m^3/s/yr)	212.4	53.0
		ΔALF_A (m^3/s/yr)	16.54	0.2
		ΔFLD_A (m^3/s)	2923.1	651.0
	Reach B	ΔRBF_B (1/d)	0.74	0.02
		ΔDHD_B (1/yr)	0.42	0.02
		ΔMFH_B (m^3/s/yr)	212.2	53.0
		ΔALF_B (m^3/s/yr)	21.34	0.3
		ΔFLD_B (m^3/s)	2818.6	528.3
	Reach C	ΔRBF_C (1/d)	0.93	0.02
		ΔDHD_C (1/yr)	0.68	0.03
		ΔMFH_C (m^3/s/yr)	441.5	58.89
		ΔALF_C (m^3/s/yr)	15.00	1.95
		ΔFLD_C (m^3/s)	2856.0	563.3

[a]Maximum and minimum values were searched with a single-objective genetic algorithm.

functions in (29) can be now rewritten as the minimization of all normalized indices:

$$\text{Minimize}\{\text{TSR}', \text{ADD}', \text{MSR}', \text{AHP}', \text{MFA}', \triangle\text{RBF}', \triangle\text{DHD}', \triangle\text{MFH}', \triangle\text{ALF}', \triangle\text{FLD}'\}. \quad (31)$$

[31] The multiobjective optimization problem posed by (31) is solved using the technique for order preference by similarity to ideal solution (TOPSIS) (see reviews on the TOPSIS by *Shiau and Wu* [2010]). The basic idea behind the TOPSIS is that the best option is the one that is least distant to the positive ideal solution (PIS) and most distant to the negative ideal solution (NIS). For operation scenarios that optimize for a single reach, the weighted total distances to the PIS and NIS, denoted as D^+ and D^-, are evaluated by

$$D^+ = \left[\sum_{i=1}^{10} w_i \left(\text{OBJ}_t' - \text{OBJ}^+\right)^2\right]^{1/2}, \quad (32a)$$

$$D^- = \left[\sum_{i=1}^{10} w_i \left(\text{OBJ}_t' - \text{OBJ}^-\right)^2\right]^{1/2}, \quad (32b)$$

where $\text{OBJ}^+ = 0$ and $\text{OBJ}^- = 1$ are PIS and NIS, respectively; w_i = weighting factor for the ith objective, by definition $\sum_{i=1}^{10} w_i = 1$; here, an equal weighting of 0.5 is assigned to the reservoir indices ($w_i = 0.1$, for $i = 1$ to 5) and environmental flow indices ($w_i = 0.1$, for $i = 6$ to 10). In this study, we tend not to assign different weights in favor of any objectives because prioritizing different objectives (human and ecosystem needs) is a decision-making problem rather than an optimization problem, thus will be left as a topic for future studies. The optimal solution is then obtained by maximizing the relative distance to the NIS D^*, which is expressed by

$$\text{Maximize}\{D^*\} = \text{Maximize}\left\{\frac{D^-}{D^+ + D^-}\right\}. \quad (33)$$

[32] In this study, the optimal solutions are searched with a simple genetic algorithm. The readers are referred to *Shiau and Wu* [2010] for more details on the genetic algorithm.

4.3. Operation Scenarios

[33] Three types of operation scenarios are considered in this study: (1) one-reach scenarios, which aim to restore the preimpact flow regime at one single reach (Reach A, B, or C); (2) two-reach scenarios, which aim to restore the natural flow regimes at two reaches (Reaches A + B, A + C, or B + C); and (3) three-reach scenario, aiming to restore the natural flow regimes at three reaches (Reaches A + B + C). Different numbers of objectives are involved in these scenarios. For one-reach scenarios (Scenarios A, B, and C), 10 objectives as shown in (31) are involved, including 5 reservoir indices and 5 environmental flow indices. The optimal solution is obtained via (33), in which the reach-based objective function D_A^*, D_B^*, or D_C^* is maximized using the environmental flow indices of Reach A, B, or C, respectively. For two-reach scenarios (Scenarios AB, AC, and BC), 15 objectives are involved, which include 5 reservoir indices and 10 environmental flow indices (5 per reach). The optimal solution is obtained by maximizing the reach-based objective function D_{AB}^*, D_{AC}^*, or D_{BC}^* using the environmental flow indices of Reaches A + B, A + C, or B + C, respectively, where a weight of 0.5 is shared among 10 environmental flow indices (i.e., $w_i = 0.05$, for $i = 6$ to 15). For the three-reach scenario ABC, 20 objectives are involved, including 5 reservoir indices and 15 environmental flow indices. The optimal solution is obtained by maximizing D_{ABC}^* using the environmental flow indices of the three reaches, where a weight of 0.5 is shared among 15 environmental flow indices (i.e., $w_i = 0.033$, for $i = 6$ to 20).

[34] For each operation scenario considered, a total of 15 decision variables are determined using the simulation-optimization approach, i.e., 2 environmental flow proportions (λ_1, λ_2), 3 three-period release parameters (γ, d_1, d_2), 3 hedging coefficients ($C_{RC}^3, C_{RC}^4, C_{RC}^5$), and 7 compelling release parameters (T_I, α_1, α_2, α_3, α_4, α_5, α_6). In these scenario simulations, the hourly reservoir inflows $Q_I^{i,j,k,l}$ and incoming flows from the Nanshih Creek $Q_N^{i,j,k,l}$

Table 3. Reach-Based Objective Functions and Optimal Results Under Different Operation Scenarios[a]

		Operation Scenario							
Category	Item	Current Rules	A	B	C	AB	AC	BC	ABC
Reach-based objective function (targeted maximal)	D^*_A	**0.644**	**0.738**[b]	0.727	0.654	0.736	0.695	0.717	0.734
	D^*_B	**0.595**	0.629	**0.665**[b]	**0.595**	0.664	0.622	0.643	0.655
	D^*_C	**0.544**	0.591	0.576	**0.663**[b]	0.583	0.648	0.628	0.610
	D^*_{AB}	**0.619**	**0.619**	0.694	0.622	**0.697**[b]	0.655	0.676	0.690
	D^*_{AC}	**0.589**	0.652	0.640	0.658	0.647	**0.670**[b]	0.667	0.662
	D^*_{BC}	**0.569**	0.609	0.616	0.627	0.620	0.634	**0.635**[b]	0.631
	D^*_{ABC}	**0.591**	0.644	0.648	0.635	0.653	0.652	0.659	**0.660**[b]
	Sum	4.15	4.48	4.57	4.45	4.60	4.58	4.63	4.64
	Overall ranking	8	6	5	7	3	4	2	1
Normalized reservoir indices (targeted minimal)	TSR′	**0.003**	0.007	0.020	**0.049**	0.012	0.029	0.017	0.008
	ADD′	0.051	0.057	**0.214**	0.157	**0.034**	0.116	0.065	0.057
	MSR′	0.114	**0.000**	0.120	**0.317**	0.121	0.141	0.098	0.022
	AHP′	**0.055**	**0.342**	0.122	0.216	0.130	0.223	0.147	0.131
	MFA′	**0.985**	0.341	0.341	**0.000**	0.335	**0.000**	0.329	0.335
	Sum	1.21	0.75	0.82	0.74	0.63	0.51	0.66	0.55
	Rank-R	8	6	7	5	3	1	4	2
Normalized reachwise environmental flow indices (targeted minimal)	Reach A $\triangle RBF'_A$	**0.078**	0.051	0.072	0.047	0.072	**0.043**	0.069	0.067
	$\triangle DHD'_A$	0.596	**0.375**	0.549	**0.767**	0.548	0.650	0.604	0.577
	$\triangle MFH'_A$	0.613	0.645	**0.574**	**0.856**	0.599	0.790	0.609	0.612
	$\triangle ALF'_A$	0.236	0.231	0.228	**0.318**	**0.206**	0.274	0.313	0.224
	$\triangle FLD'_A$	**0.202**	**0.008**	0.054	0.182	0.040	0.162	0.067	0.017
	Sum	1.73	1.31	1.48	2.17	1.47	1.92	1.66	1.50
	Rank-A	6	1	3	8	2	7	5	4
	Reach B $\triangle RBF'_B$	0.059	**0.046**	**0.060**	0.048	**0.060**	0.048	0.058	0.058
	$\triangle DHD'_B$	0.638	0.801	**0.629**	**0.889**	0.644	0.837	0.713	0.681
	$\triangle MFH'_B$	0.614	0.646	**0.575**	**0.857**	0.599	0.791	0.610	0.613
	$\triangle ALF'_B$	0.844	0.852	**0.746**	0.874	0.783	0.842	**0.896**	0.858
	$\triangle FLD'_B$	**0.158**	0.019	**0.010**	0.156	0.042	0.151	**0.010**	0.018
	Sum	2.31	2.36	2.02	2.82	2.13	2.67	2.29	2.23
	Rank-B	5	6	1	8	2	7	4	3
	Reach C $\triangle RBF'_C$	0.130	0.199	**0.384**	**0.037**	0.371	0.059	0.082	0.111
	$\triangle DHD'_C$	**0.760**	0.648	0.695	**0.209**	0.710	0.359	0.525	0.647
	$\triangle MFH'_C$	**0.983**	0.967	0.951	**0.929**	0.960	0.938	0.958	0.967
	$\triangle ALF'_C$	**1.000**	0.991	0.990	**0.676**	0.995	0.830	0.856	0.958
	$\triangle FLD'_C$	**0.158**	0.019	**0.010**	0.155	0.042	0.151	**0.010**	0.018
	Sum	3.03	2.82	3.03	2.01	3.08	2.34	2.43	2.70
	Rank-C	7	5	6	1	8	2	3	4
Decision variables (operational parameters)	λ_1 (−)	0[c]	0	0	0.42	0	0.22	0.16	0.04
	λ_2 (−)	0[c]	0.02	0.02	0	0.01	0	0	0.01
	γ (−)	1[c]	0.56	0.90	0.90	0.89	0.85	0.90	0.90
	d_1 (h)	8[c]	12	7	10	7	10	8	8
	d_2 (h)	8[c]	5	8	10	8	10	8	8
	C^3_{RC}(−)	1[c]	1	0.9	1	1	1	1	1
	C^4_{RC}(−)	0.9[c]	0.82	0.70	0.70	0.70	0.70	0.73	0.80
	C^5_{RC}(−)	0.7[c]	0.82	0.81	0.54	0.69	0.70	0.73	0.80
	T_I (m^3/s)	400[c]	220	200	490	220	210	290	290
	α_1 (−)	0.5[c]	0.51	0.43	0.46	0.51	0.51	0.49	0.56
	α_2 (−)	0.2[c]	0.36	0.38	0.26	0.34	0.35	0.39	0.39
	α_3 (−)	0.8[c]	0.70	0.73	0.90	0.73	0.90	0.77	0.70
	α_4 (−)	0.6[c]	0.55	0.70	0.57	0.56	0.55	0.70	0.51
	α_5 (−)	0.4[c]	0.37	0.32	0.34	0.30	0.36	0.34	0.38
	α_6 (m^2/s)	100[c]	200	190	170	200	200	190	200

[a]Bold figures are the most superior or inferior results among all the values of an objective/index associated with different scenarios.
[b]Reach-based objective function is optimal only when the reaches included in the operation scenario match the reaches (in subscript) that are used to calculate the objective function.
[c]Specified values (not determined by optimization).

(1998−2008) are used as the input flow series. The hourly reservoir releases, weir diversions, and postimpact flows at the three study reaches are the outputs of the scenario simulations.

5. Results and Discussion

[35] The optimal operational parameters derived under the different operation scenarios, along with the specified parameter values for the current operation rules, are summarized in Table 3. Under the current operation rules, the environmental flow proportions λ_1 and λ_2 are both set to be 0. The flow releases for the domestic water supply and peaking hydropower generation are implemented in the same period ($\gamma = 1$, $d_1 = d_2 = 8$ h). Shown in Figure 5 are the reachwise hourly flows at Reaches A to C resulting from different operation scenarios, during 17−20 February 2006 (partially overlapped with the period shown in Figure 3).

Table 4. Hydropower Generation Characteristics of Feitsui Reservoir

Reservoir Water Level, EL_F (m)	Reservoir Storage, S_F (10^6 m^3)	Efficiency, η (%)	Effective Head, H_E (m)	Design Discharge, Q_{DP} (m^3/s)
170	384.95	88.53	111.35	72.5
165	341.66	89.61	106	75.2
155	261.15	91.38	96	81.5
148.3	213.58	92.56	89	86.7
140.8	167.88	92.95	81	94.9
133.4	131.33	90.92	73.8	91.3
130	115.01	89.06	70.55	90.2
125	95.95	86.62	65.7	87.5
120	76.88	83.69	60.85	84.2
117.1	68.72	81.76	58	82.5

Under the current operation rules, the daily flow hydrographs at these reaches exhibit similar repetitive 8 h peak patterns. The surplus peak discharges observed at Reach C arise from the releases for peaking hydropower generation that exceed the domestic water demands.

[36] Under different operation scenarios, the environmental flow proportions λ_1 and λ_2 vary with the reach considered (Table 3). For those scenarios considering Reach C (scenarios C, AC, and BC), the environmental flows are supported solely by the Nanshih Creek ($\lambda_1 \neq 0$, $\lambda_2 = 0$), while for those excluding Reach C (scenarios A, B, and AB), the environmental flows are supplied solely by the Peishih Creek ($\lambda_1 = 0$, $\lambda_2 \neq 0$). However, for scenario ABC that incorporates all reaches, the environmental flows are supported by both creeks ($\lambda_1 \neq 0$, $\lambda_2 \neq 0$). Such results highlight the spatial control imposed by the proposed environmental flow strategy. Since the environmental flow proportion λ_1 is controlled by weir diversions, the scenarios incorporating Reach C would rely on λ_1; the environmental flow proportion λ_2 is controlled by reservoir releases; hence, the scenarios incorporating Reaches A and B would rely on λ_2. In general, λ_1 is $>$ λ_2, which indicates that Reach C, categorized as a reach with reduced discharge, demands more environmental flows than those required by Reaches A and B, where flows are regulated but not reduced by reservoir operations.

[37] For scenario A, d_1 ($=$12 h) is $>>$ d_2 ($=$ 5 h), resulting in a distinct three-period release scheme (Figure 5). Similar to the results under the current operation rules, the surplus peaks observed at Reach C are due to the flow releases for hydropower generation that exceed the demands for domestic water supply. For scenarios B and AB, d_2 ($=$ 8 h) is 1h $>$ d_1 ($=$ 7 h), resulting in the spikes observed at Reach C at the eighth hour of the surplus peaks (Figure 5c). For scenarios C and AC, d_1 and d_2 overlap in the same 10 h, making it a two-period (peak and off-peak) release scheme (Figure 5). The differences between these two scenarios are the release and environmental flow proportions ($\gamma = 0.9$ versus 0.85 and $\lambda_1 = 0.42$ versus 0.22), leading to slightly smaller off-peak flows for scenario C at Reaches A and B (Figures 5a and 5b). At Reach C (Figure 5c), however, the off-peak flows for scenario C are more than those associated with scenario AC mainly due to the greater value of λ_1 with scenario C, while the surplus peaks for scenario C are less than those associated with scenario AC due to the greater diversions during peak periods. These differences between peak and off-peak diversions arise from the operation rules given in (11) and (5), which work to secure that the daily domestic demands are met by each operation scenario.

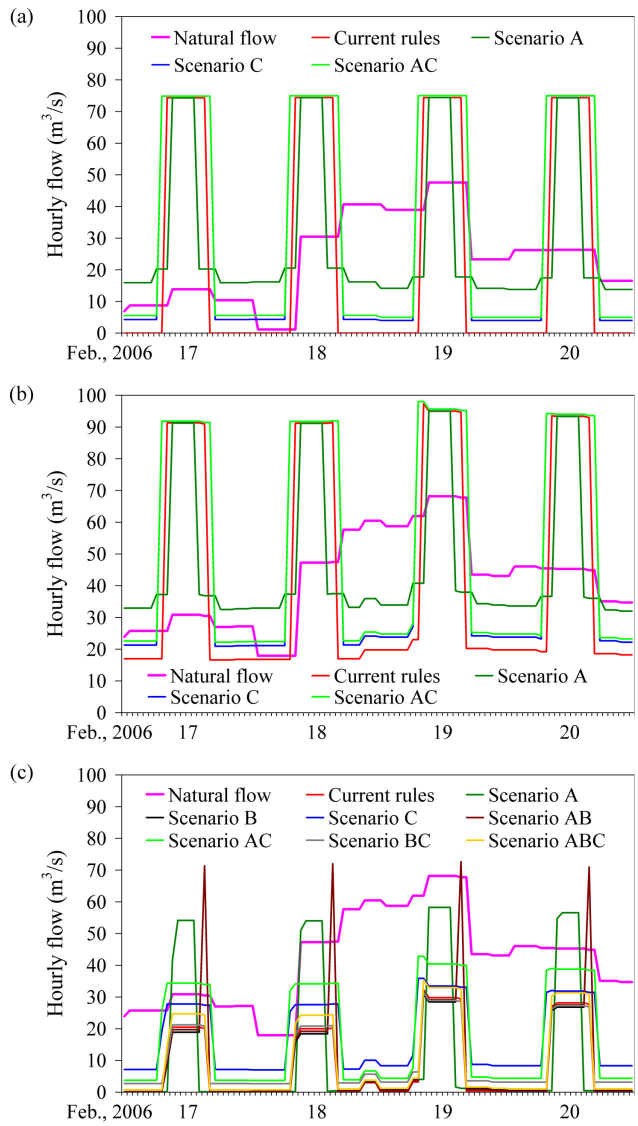

Figure 5. Hourly flows (17–20 February 2006) under different scenarios at Reaches (a) A, (b) B, and (c) C. In Figures 5a and 5b, scenarios B/AB are not shown due to overlap with current operation rules, and scenarios BC/ABC are not shown due to overlap with scenario B.

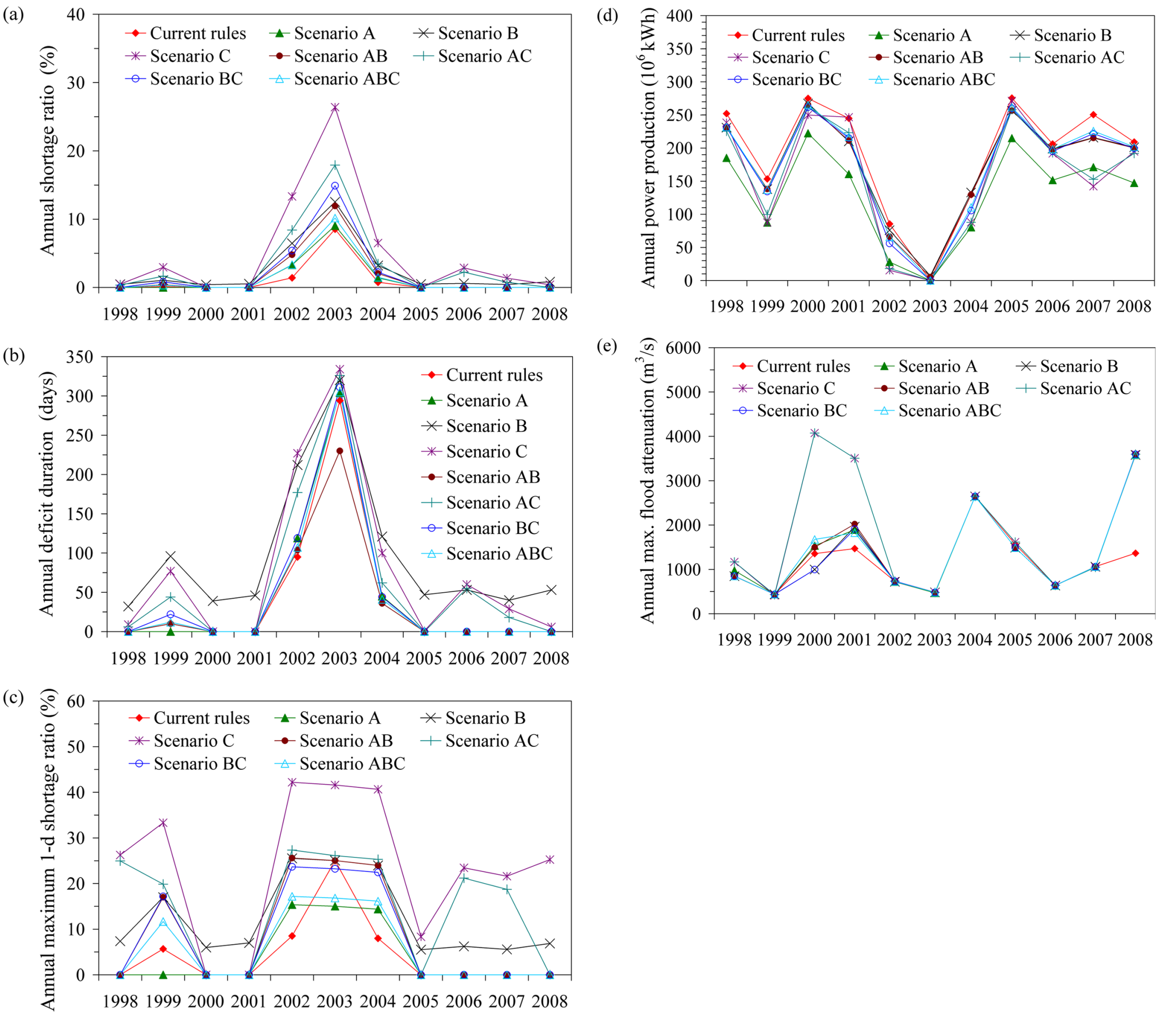

Figure 6. Annual values of reservoir indices resulting from different operation scenarios: (a) shortage ratio, (b) deficit duration, (c) maximum 1 day shortage ratio, (d) hydropower production, and (e) maximum flood attenuation.

[38] For scenarios BC and ABC, the release periods d_1 and d_2 overlap in the same 8 h as with the current operation rules. The main difference between these two scenarios is the environmental flow proportions. For scenario BC ($\lambda_1 = 0.16$, $\lambda_2 = 0$), environmental flows are supported solely by the Nanshih Creek; while for scenario ABC ($\lambda_1 = 0.04$, $\lambda_2 = 0.01$), environmental flows are supplied by both creeks. Similar to those with scenarios C and AC, the postdiversion flows at Reach C (Figure 5c) reveal that the off-peak flows for scenario BC are more than those associated with scenario ABC due to the much greater λ_1 value of scenario BC, while the surplus peaks of scenario BC are less than those of scenario ABC due to the greater peak-period diversions.

[39] In the following sections, the optimal outcomes (i.e., reservoir and environmental flow performances) associated with different operation scenarios are presented and discussed.

5.1. Reservoir Performances Under Different Operation Scenarios

[40] To show the optimal reservoir performances under different operation scenarios, the annual values of the five reservoir indices are given in Figure 6. The annual shortage ratios are normally <5% but can be >10% in drought years (Figure 6a). Scenario C nearly always leads to the highest shortage ratios, whereas the current operation scheme is associated with the lowest values. This is also evident in Table 3, where the normalized total shortage ratio (TSR′) of Scenario C (= 0.049) is the most inferior, while the TSR′ value under the current operation rules (= 0.003) is the most superior. Since Scenario C is aimed at optimizing the environmental flow objectives of Reach C, such result highlights the conflicting demands that typically pose challenges for water allocation at a diversion weir. The current operation rules, which aim to meet human demands without considering the environmental flow demands, however, secure the minimum deficit of water supplied to the domestic users.

[41] The annual deficit durations are normally <100 days but can be >200 days in drought years (Figure 6b). Scenarios B and C are the two scenarios that result in the longest deficit durations whereas Scenario AB and the current operation scheme are the two leading to the shortest deficit durations. This is also shown in Table 3, where the

normalized mean annual deficit durations (ADD$'$) of Scenarios B and C (= 0.214 and 0.157) are the most inferior, while the ADD$'$ values resulting from Scenario AB and the current operation rules (= 0.034 and 0.051) are the most superior. Note that Scenarios AB and B result in the smallest and largest ADD$'$ values, respectively, despite very similar operational parameters. The reason for this lies in the value of $C^3_{\mathrm{RC}} (= 0.9)$ associated with Scenario B. This C^3_{RC} value would enact a 10% hedging policy while the others still implement a full release policy ($C^3_{\mathrm{RC}} = 1$). On the other hand, the reason that Scenario AB outperforms the current operation rules lies in the values of C^4_{RC}. The C^4_{RC} value of Scenario AB (= 0.7) would enact a 30% hedging policy while the current operation scheme ($C^4_{\mathrm{RC}} = 0.9$) only enacts a 10% hedging policy. The greater limitation on the flow releases that is associated with Scenario AB would act to secure a larger amount of water storage available for subsequent water supplies, leading to the shorter deficit durations but at the cost of greater shortage ratios.

[42] The annual maximum 1 day shortage ratios are normally <30%, with the only exception observed with Scenario C (Figure 6c). This is also evident in Table 3, where the MSR$'$ value of Scenario C (= 0.317) is the most inferior, while the MSR$'$ value of Scenario A (= 0) is the most superior. Because the maximum 1 day shortage ratio is a measure that quantifies the extreme deficit condition, it is strongly affected by the hedging policy imposed, particularly by C^5_{RC} that governs the flow release reduction during the period when the reservoir storage is below the critical rule curve. The most superior and inferior MSR$'$ values associated with Scenarios A and C are, respectively, due to their highest and lowest C^5_{RC} values (= 0.82 and 0.54), which would, respectively, enact an 18% and 46% hedging policy at the critical stage.

[43] The annual power productions (Figure 6d) under different operation scenarios exhibit similar trends. The current operation rules consistently outperform other scenarios, while Scenario A is for most of the time the least productive one. This is also observed in Table 3, where the AHP$'$ resulting from the current operation scheme (= 0.055) is the most superior, while the AHP$'$ value of Scenario A (=0.342) is the most inferior. Such results are mainly attributed to the release period d_2 assigned to the peaking hydropower generation. For the current operation rules, the release period d_2 (= 8 h) overlaps with the release period d_1 for the domestic water supply, while the release period d_2 (= 5 h) of Scenario A is the shortest among all.

[44] The annual maximum flood attenuations under Scenarios C and AC are consistently the largest ones, while the annual maximum flood attenuations resulting from the current operation rules are almost invariably the smallest ones (Figure 6e). These are also shown in Table 3, where the normalized maximum flood attenuations MFA$'$ of Scenarios C and AC (= 0) are the most superior ones, while the MFA$'$ resulting from the current operation rules (= 0.985) is the most inferior among all. Such results are mainly attributed to the large λ_1 values of Scenarios C and AC (= 0.42 and 0.22) aiming to optimize the environmental flow objectives of Reach C. The greater environmental flow proportion λ_1 of the Nanshih Creek would require a greater amount of reservoir releases to supplement domestic water supplies, thus would leave more space available for flood attenuation. The zero values of λ_1 and λ_2 under the current operation rules would retain the largest storage of water in the reservoir but the least space available for flood attenuation.

[45] The sum of all normalized reservoir indices is used here to evaluate the subranking of an operation scenario in reservoir performance, which is denoted as Rank-R and shown in Table 3, where an operation scenario that has the smallest sum would be ranked as the first. In general, the two- and three-reach scenarios have the better reservoir performance (ranked as top 4), followed by one-reach scenarios (ranked as the fifth to seventh). The current operation scheme (ranked as the eighth), although excels in TSR$'$ and AHP$'$, does not perform as well as expected, mainly due to the poor performance in MFA$'$. These results imply that taking into account the environmental flow demands does not necessarily degrade the overall reservoir performance. This is especially true when the environmental flow objectives of two or three reaches are incorporated in the reservoir operation scheme because regular environmental flow releases would have positive effects on flood control, which in turn would compensate for the adverse effects on domestic water supply and hydropower generation.

5.2. Environmental Flow Performances at Different Temporal Scales

5.2.1. Environmental Flow Performances at Subdaily Timescale

[46] In this section, we present the reachwise environmental flow performances at subdaily timescale under different operation scenarios. At Reach A, the postimpact annual values of RBF resulting from different operation scenarios appear to be similar (Figure 7a). Scenario AC is the most efficient one in restoring the preimpact subdaily flow flashiness, whereas the postimpact annual RBF values resulting from the current operation rules are the most dissimilar ones to the preimpact RBF. The extremely low RBF associated with Scenario A in 2003 (drought year) is mainly attributed to the most evenly distributed flow release parameters $\gamma = 0.56$ and $d_1 = 12$ h, which lead to the smallest subdaily flashiness particularly during the drought periods when no flows are released for peaking hydropower generation. Consistent results are shown in Table 3, where the $\triangle\mathrm{RBF}'_A$ value resulting from Scenario AC (= 0.043) is the most superior one among all, while the $\triangle\mathrm{RBF}'_A$ value resulting from the current operation rules (= 0.078) is the most inferior one.

[47] At Reach B, the postimpact annual RBF values resulting from all operation scenarios are similar (Figure 7b). The postimpact subdaily flashiness resulting from Scenario A is the most similar one to the natural condition. This is also evident in Table 3, where the $\triangle\mathrm{RBF}'_B$ value of Scenario A (= 0.046) is the most superior one among all, while the $\triangle\mathrm{RBF}'_B$ values of Scenarios B and AB (= 0.060) are the most inferior ones among all. Overall, the subdaily flashiness of Reach B is the least altered compared to the postimpact RBF of Reaches A and C (Figures 7a and 7c), which is attributed to the unregulated, dominant incoming flows from the Nanshih Creek.

[48] At Reach C, the postimpact RBF values resulting from different operation scenarios exhibit rather different results (Figure 7c). The postimpact RBF values of

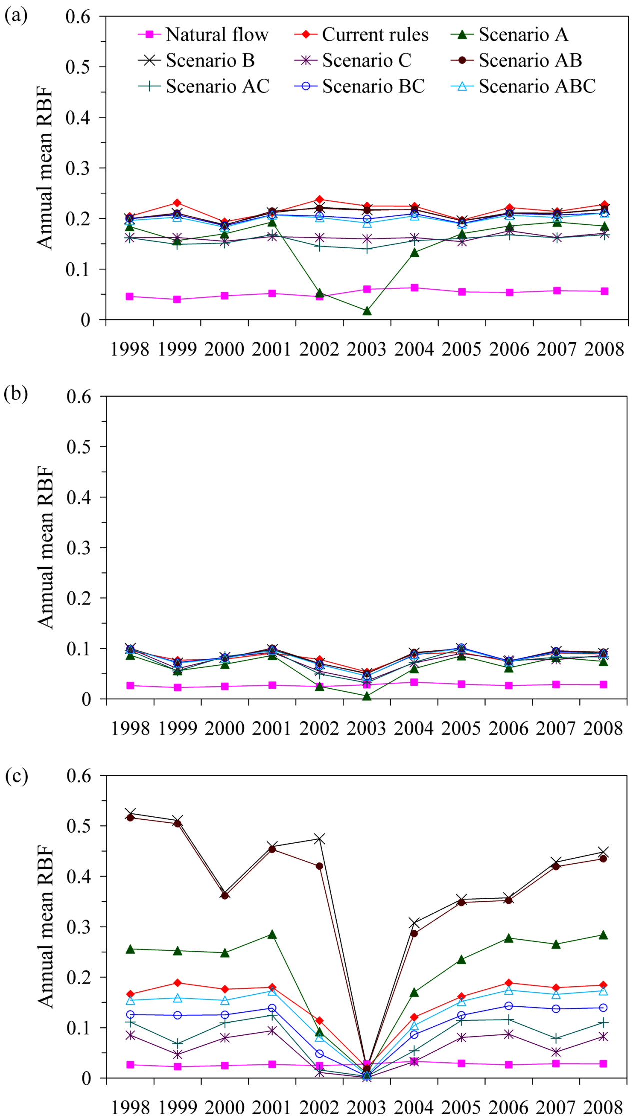

Figure 7. Annual mean values of RBF (subdaily-scale environmental flow index) resulting from different operation scenarios at (a) Reach A, (b) Reach B, and (c) Reach C.

Scenario C are consistently the most similar ones to the natural RBF while the postimpact RBF values of Scenario B are invariably the least similar ones to the natural RBF. This is also observed in Table 3, where the $\triangle RBF'_C$ values of Scenario C (= 0.037) and Scenario B (= 0.384) are the most superior and inferior ones among all, respectively. Operation scenarios considering Reach C (Scenarios C, AC, BC, and ABC) are all superior to the current operation rules, whereas those that exclude Reach C (Scenarios A, AB, and B) are all inferior to the current operation rules, which reveal the significant impacts of weir diversions and highlight the mitigation effects achieved by including Reach C in the environmental flow objectives.

5.2.2. Environmental Flow Performances at Daily Timescale

[49] The postimpact daily flow variability (Figure 8) is mainly affected by environmental flow releases, in contrast to the postimpact subdaily flashiness (Figure 7) that is primarily influenced by the releases for domestic water supply and peaking hydropower generation. Take Scenario A (which aims to optimize the environmental flow objectives of Reach A) as an example, whose postimpact DHD values are the most similar ones to the natural status among all (Figure 8a). This is also true for Scenarios B and C, whose postimpact DHD values (Figures 8b and 8c) are, respectively, the most similar ones to the preimpact DHD of Reaches B and C. Similar results are also seen in Table 3, where the $\triangle DHD'_A$ value of Scenario A (= 0.375), the $\triangle DHD'_B$ of Scenario B (= 0.629), and the $\triangle DHD'_C$ of Scenario C (= 0.209) are consistently the optimal reach-wise values of the daily-scale environmental flow index.

[50] At Reaches A and B (Figures 8a and 8b), the postimpact DHD of all operation scenarios are consistently less than the preimpact DHD, while, at Reach C (Figure 8c), the postimpact DHD are consistently more than the preimpact DHD, indicating that daily-flow variability is increased due to weir diversions. Such effect is most significant for those

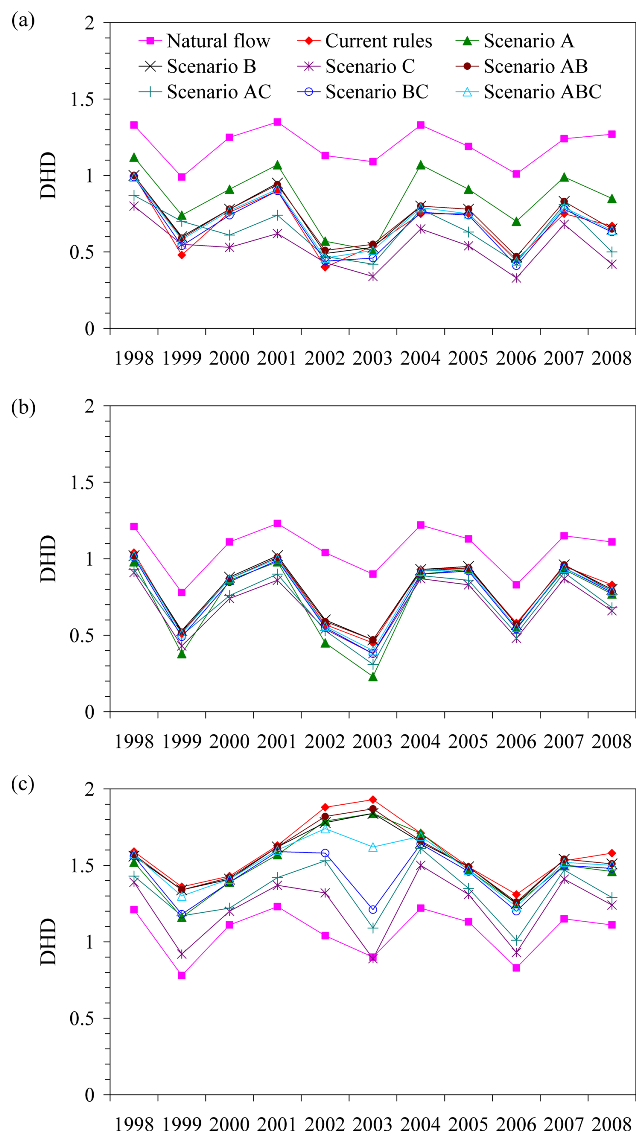

Figure 8. Annual values of DHD (daily-scale environmental flow index) resulting from different operation scenarios at (a) Reach A, (b) Reach B, and (c) Reach C.

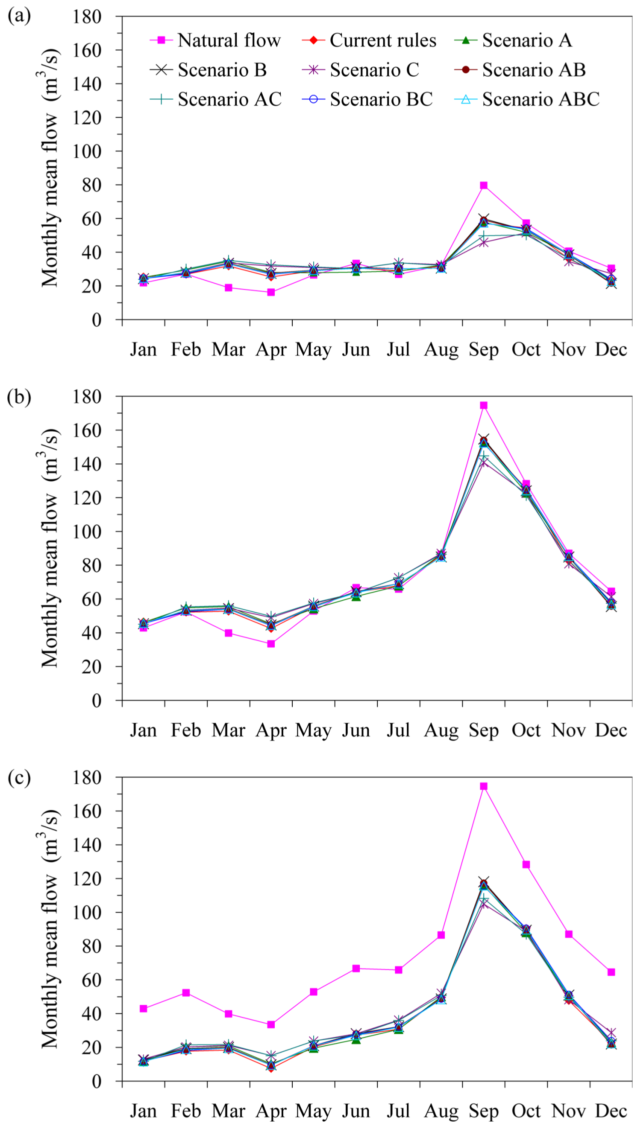

Figure 9. Monthly mean flows (seasonal-scale wet and dry patterns) resulting from different operation scenarios at (a) Reach A, (b) Reach B, and (c) Reach C.

scenarios that do not incorporate Reach C in the environmental flow objectives (Scenarios A, B, and AB), whose postimpact DHD values peak in 2003 (drought year), in contrast to the decreased DHD resulting from other scenarios that incorporate Reach C in the optimization (Scenarios C, AC, BC, and ABC).

5.2.3. Environmental Flow Performances at Seasonal Timescale

[51] At Reaches A and B, the postimpact monthly flows show no substantial deviations from the preimpact ones (Figures 9a and 9b), while at Reach C, the postimpact monthly flows deviate from the preimpact ones by the flow offsets caused by weir diversions (Figure 9c), although no significant difference between the postimpact hydrographs is observed at any reach. For Reaches A and B, more apparent deviations from the preimpact monthly flows are observed in March/April (dry season) and September (flood season), during which flow releases for domestic water supplies/hydropower generation would increase the dry-season monthly flows while the flood attenuation measures would lower the flood-season monthly flows. The impact of weir diversions is slightly mitigated when Reach C is included in the environmental flow objectives, as observed in Table 3, where the reachwise seasonal-scale index $\triangle \mathrm{MFH}'_C$ of Scenario C (= 0.929) is the optimal one among all scenarios.

5.2.4. Environmental Flow Performances at Annual Timescale

[52] Figure 10 shows the reachwise annual low flows under different operation scenarios, where the differences among the three reaches are clearly demonstrated. Since Reach A is located immediately downstream of the reservoir, the annual low flows at Reach A are the direct consequences of the operation scheme imposed (Figure 10a). The uncertainties of the postimpact low flows relative to the preimpact ones arise from the flow releases that are governed by not only the human demands but also the reservoir storage and incoming flows from the Nanshih Creek.

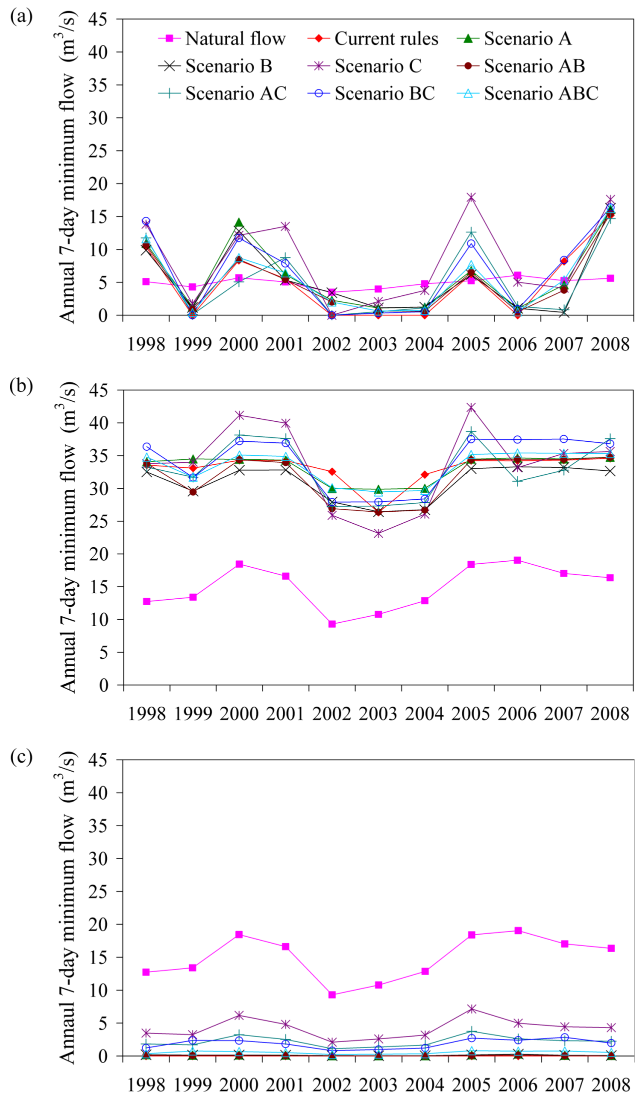

Figure 10. Annual 7 day minimum (annual-scale low) flows resulting from different operation scenarios at (a) Reach A, (b) Reach B, and (c) Reach C.

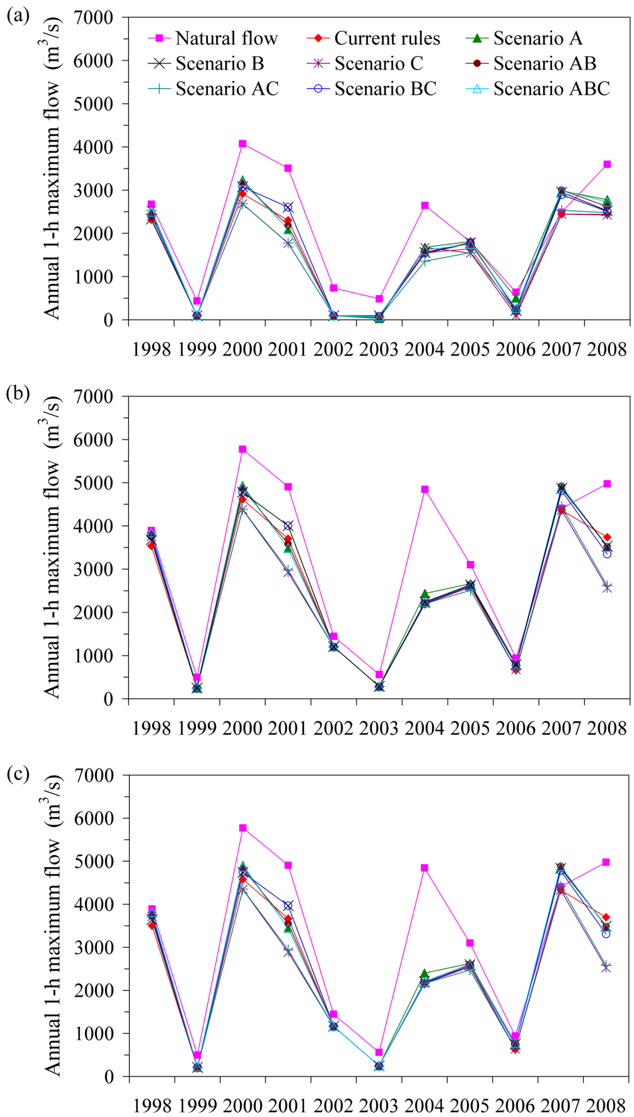

Figure 11. Annual 1 h maximum flows (from which interannual-scale large floods are derived) resulting from different operation scenarios at (a) Reach A, (b) Reach B, and (c) Reach C.

The zero annual low flows would occur when the incoming flows from the Nanshih Creek are sufficient for domestic water supply without a need of reservoir releases; meanwhile, the reservoir water level is less than the threshold for hydropower generation and no environmental flow releases are implemented ($\lambda_2 = 0$).

[53] At Reach B, the postimpact annual low flows under different operation scenarios are, however, consistently more than the natural ones (Figure 10b). Given that flows at Reach B are the sum of incoming flows from Reach A and Nanshih Creek, such kind of consistently greater postimpact annual low flows imply that the postimpact annual low flows at Reach A are out of phase with the annual low flows coming from the Nanshih Creek; it is primarily the reservoir releases that contribute to raise the annual low flows at Reach B. In contrast, at Reach C, the postimpact annual low flows resulting from different operation scenarios are invariably less than the natural ones (Figure 10c). Since Reach C is located below the diversion weir, the invariably smaller postimpact annual low flows, particularly the zero flows under the current operation rules, demonstrate clearly the impacts of weir diversions.

[54] The reachwise values of annual-scale environmental flow index $\Delta ALF'$ resulting from different operation scenarios are shown in Table 3, where the reachwise $\Delta ALF'$ values tend to be optimal when the reach in question is included in the operation scenario. For example, the $\Delta ALF'_B$ value of Scenario B ($= 0.746$) is the optimal one among all $\Delta ALF'_B$, and the $\Delta ALF'_C$ value of Scenario C ($= 0.676$) is the optimal one among all $\Delta ALF'_C$. The $\Delta ALF'_A$ value of Scenario A ($= 0.231$), although suboptimal, is ranked as the top four among all $\Delta ALF'_A$, which again highlights the inherent uncertainties associated with the postimpact annual low flows at Reach A.

5.2.5. Environmental Flow Performances at Interannual Timescale

[55] The reachwise annual 1 hour maximum flow series under different operation scenarios are shown in Figure 11, where the postimpact annual extreme flow series resulting from all operation scenarios appear to be similar, which coincides with the previous finding that the flood-related environmental flow objectives are unlikely further improved by modifying the operation schemes [*Shiau and Wu*, 2010]. In general, the postimpact annual extreme flows are less than the natural ones thanks to the flood control measures. However, the natural temporal pattern of interannual large floods is retained by the postimpact flows at all study reaches, where a similar recurrence interval of interannual large floods is exhibited.

[56] The reachwise values of interannual-scale environmental flow index $\Delta FLD'$ under different operation scenarios are shown in Table 3, where the reachwise $\Delta FLD'$ values also tend to be optimal when the reach in question is incorporated in the operation scenario. For example, the $\Delta FLD'_A$ value of Scenario A ($= 0.008$) is the optimal among all $\Delta FLD'_A$ values, and the $\Delta FLD'_B$ value of Scenario B ($= 0.010$) is the optimal among all $\Delta FLD'_B$ values. The $\Delta FLD'_C$ values are, however, nearly identical to their counterpart $\Delta FLD'_B$ values, implying that the weir diversions become negligible compared to the interannual-scale large floods.

5.3. Reachwise Environmental Flow Performances Under Different Scenarios

[57] For an operation scenario, the sum of all normalized environmental flow indices of a reach is used here to define the reachwise subranking of that scenario in environmental flow performance, denoted as Rank-A, Rank-B, and Rank-C for Reaches A, B, and C, respectively. The reachwise subrankings of different operation scenarios are shown in Table 3, where the reachwise subranking of a one-reach scenario that considers the corresponding reach in question will outrank those of other scenarios. Specifically, Scenario A is ranked as the first in Rank-A, Scenario B is ranked as the first in Rank-B, and similarly Scenario C is ranked as the first in Rank-C. However, a mutual exclusion is observed between Scenario C and Scenario A, B, or AB. For instance, Scenario C is ranked as the eighth (last) in Rank-A and Rank-B, indicating that the excess flow releases from the reservoir that aim to restore the natural

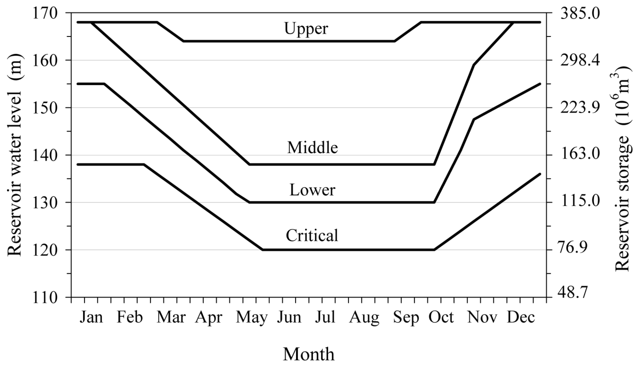

Figure 12. Operational rule curves of Feitsui Reservoir. Reservoir storage level is divided into five zones by four rule curves.

flow regime below the diversion weir (Reach C) would deteriorate the flow regimes above the diversion weir (Reaches A and B). Similarly, Scenarios A, B, and AB are ranked as the fifth, sixth, and eighth, respectively (last four), in Rank-C. This mutual exclusion between the reaches above and below a diversion weir redefines the conventional perception that restoring the flow regime of a downstream reach would automatically restore those of the upstream reaches. For example, *Shiau and Wu* [2010] select the lowermost reach as a target for achieving the basin-scale flow restoration, assuming that the hydrological impacts of the impoundment and diversion facilities on the upper reaches can be simultaneously mitigated. Our results suggest that such assumption may not be generally valid especially when there are flow diversions. The current operation scheme, without considering the environmental flow needs, invariably ranks among the last four in the environmental flow performance (ranked as the sixth, fifth, and seventh in Rank-A, Rank-B, and Rank-C, respectively).

5.4. Overall Evaluation of Different Operation Scenarios

[58] For an operation scenario, the sum of all reach-based objective functions $D_A^*, D_B^*, D_C^*, D_{\mathrm{AB}}^*, D_{\mathrm{AC}}^*, D_{\mathrm{BC}}^*$, and D_{ABC}^* is used to evaluate the overall performance of that scenario under all combinations of reaches, denoted as Overall Ranking in Table 3, where the reach-based objective function is optimal only when the reaches incorporated in the operation scenario match the reaches (subscript) that are used to calculate the objective function. For example, D_{AB}^* is optimal under Scenario AB but is suboptimal under other scenarios. In the light of the overall rankings, the three-reach scenario ABC (ranked as the first) outperforms the two-reach scenarios BC, AB, and AC (ranked as the second, third, and fourth, respectively), which then outperform the one-reach scenarios B, A, and C (ranked as the fifth, sixth, and seventh, respectively) and the current operation rules (ranked as the last). Despite that Scenario ABC never stands out as the first rank in any reservoir/environmental flow indices, it, nevertheless, always remains as the top four in all subrankings (ranked as the second, fourth, third, and fourth in Rank-R, Rank-A, Rank-B, and Rank-C, respectively), and unlike other scenarios, it never ranks among the last four in any of the subrankings. The consistent, stable performances of Scenario ABC are the key to the top overall ranking. In contrast, the reach-based objective functions associated with the current operation rules are invariably the most inferior ones, which is mainly attributed to the most inferior Rank-R (section 5.1) and poor subrankings in the reachwise environmental flow performance (ranked as the sixth, fifth, and seventh in Rank-A, Rank-B, and Rank-C, respectively).

[59] As an alternative option from the one- or two-reach scenarios, our results suggest that the operation scenario that incorporates Reach B (i.e., Scenario B, BC, or AB) may be taken. Scenario B, by aiming to restore the flow regime of Reach B, benefits also the flow regime of the upstream Reach A (Scenario B is ranked as the third in Rank-A). Scenario BC or AB, in addition to restoring the flow regime of Reach B, benefits also the flow regime of the downstream Reach C (Scenario BC is ranked as the third in Rank-C) or upstream Reach A (Scenario AB is ranked as the second in Rank-A).

6. Conclusions

[60] We tackle in this study the temporal and spatial problems associated with the optimal environmental flow and operation strategies for a multipurpose reservoir system. We use a novel environmental flow proportion strategy and three-period release approach, and the multireach operation scenarios to optimize simultaneously the reservoir performances and environmental flow objectives at subdaily to interannual timescales for a maximum of three connected reaches. The results obtained with our simulation-optimization framework imply that taking into account the environmental flow demands does not necessarily degrade the overall reservoir performance. This is particularly true if the environmental flow objectives of two or three reaches are included in the operation scheme because regular environmental flow releases would have positive effects on flood control, which in turn would compensate for the adverse effects on domestic water supply and hydropower generation.

[61] The proposed three-period release approach restores mainly the subdaily flow regime, while the environmental flow proportion strategy restores primarily the daily flow regime. The annual extreme flow series resulting from all operation scenarios are similar, consistent with our previous finding that the flood-related environmental flow objectives are unlikely further improved by modifying the operation rules. Spatially, a mutual exclusion is observed between the reaches above and below a diversion weir, which revises the perceived notion that restoring the downstream flow regime would automatically restore those at upstream.

[62] An overall evaluation reveals that the three-reach scenario outperforms the two-reach ones, which then outperform the one-reach ones. Although the three-reach scenario is never ranked as the first in any reservoir or environmental flow indices, the consistent and stable performances of this scenario are the key to the top overall ranking. The one- or two-reach scenarios that incorporate the midstream reach in the operation strategy may be taken as an alternative option because such scenarios would benefit the upstream or downstream reach in addition to the midstream reach.

[63] Despite that the results reported in this paper are derived from a case study concerning the Feitsui Reservoir system in Taiwan, the conclusions and implications presented here are general and applicable to other multipurpose reservoir systems. In particular, the proposed environmental flow and reservoir release strategies and the multireach operation scenarios, along with the integrated simulation-optimization framework, provide a practical approach to address the complex temporal/spatial issues in regard to the operations of multipurpose reservoir systems that take into account both the human and ecosystem demands. However, the ecosystem responses to hydrologic alterations and the ecological assets other than rivers (e.g., wetlands and floodplains) [*Higgins et al.*, 2011; *Szemis et al.*, 2012] are not considered in this work and remain as directions for further extending this research.

Notation and Abbreviation

$A^{i,j,k,l}$	hourly reservoir surface area (km^2).
ADD	mean annual deficit duration (d).
AHP	mean annual hydropower production (kWh/yr).
ALF^i	annual 7 days minimum flow (m^3/s).
C_{RC}	release coefficient for domestic water supply.
$D^{i,j,k}$	projected daily domestic demand (m^3/d).
D^+, D^-	weighted total distances to PIS and NIS (−).
D^*, $D^*_{A\sim \mathrm{ABC}}$	relative distance to D^-(−), and reach-based objective functions (−).
d_1, d_2	release periods for domestic water supply and hydropower generation (h)
DHD	daily hydrograph dissimilarity index.
$\mathrm{DR}^{i,j,k}$	daily release for domestic water supply (m^3/d).
$\mathrm{DWS}^{i,j,k}$	daily water shortage (m^3/d).
$E^{i,j,k,l}$, $e^{i,j,k}$	hourly evaporation loss (m^3), and daily evaporation rate (mm/d).
$\mathrm{EL}_F^{i,j,k,l}$	hourly reservoir water level (m).
FLD_5	5 year flood (m^3/s).
H_E	effective head for hydropower generation (m).
(l_1, l_2), (l_3, l_4)	starting and ending hours of release periods d_1 and d_2 (h).
MFA, MSR	maximum flood attenuation (m^3/s), and maximum 1 day shortage ratio (%).
N_j, N_Y	number of days in the *j*th month, number of years over the study period.
OBJ_i, OBJ'_i	original value (units see Table 2) and normalized value of the *i*th index.
OBJ^+, OBJ^-	PIS (= 0) and NIS (= 1).
PIS, NIS	positive and negative ideal solutions, respectively.
$Q_M^{i,j,k,l}$	hourly flow at Reach M (m^3/s).
Q_{DP}	design discharge for hydropower generation (m^3/s).
$Q_{\mathrm{DV}}^{i,j,k,l}$	hourly weir diversion rate (m^3/s).
$Q_I^{i,j,k,l}$	hourly reservoir inflow (m^3/s).
$Q_I^{i,m,l}$	hourly reservoir inflow on the *m*th Julian day (m^3/s).
$Q_N^{i,j,k,l}$	hourly incoming flow from the Nanshih Creek (m^3/s).
$R_D^{i,j,k,l}$	hourly reservoir release rate for domestic water supply (m^3/s).
$R_{\mathrm{EF}}^{i,j,k,l}$	hourly reservoir release rate for environmental flow (m^3/s).
$R_{\mathrm{FL}}^{i,j,k,l}$	hourly compelling release rate for flood control (m^3/s).
$R_{\mathrm{HP}}^{i,j,k,l}$	hourly reservoir release rate for hydropower generation (m^3/s).
$R_{\mathrm{SP}}^{i,j,k,l}$	hourly reservoir spill (m^3/s).
$R_T^{i,j,k,l}$	hourly total reservoir release rate (m^3/s).
Rank-M	reachwise subranking in environmental flow performance (for Reach M).
Rank-R	subranking in reservoir performance.
RBF	Richards-Baker flashiness index.
$\mathrm{RC}^{j,k}$	daily rule curve values (m).
$S_C^{i,j,k,l}$, $S_F^{i,j,k,l}$	hourly weir and reservoir storages (m^3).
$S_C^{\max}$, $S_F^{\max}$	capacities of the Chingtan Weir and Feitsui Reservoir (m^3).
$S_F^{\min}$	dead storage of the Feitsui Reservoir (m^3).
T_I	threshold of reservoir inflow for triggering compelling release (m^3/s).
TFRA	Taipei Feitsui Reservoir Administration.
TOPSIS	Technique for Order Preference by Similarity to Ideal Solution.
TPC	Taiwan Power Company.
TSR	long-term total shortage ratio (%).
w_i	weighting factor of the *i*th objective (−).
$\alpha_{1\sim6}$	compelling release coefficients (units see Table 3).
ΔALF	mean difference between pre- and postimpact annual low flows (m^3/s/yr).
ΔDHD	mean difference between natural and altered DHD values (1/yr).
ΔFLD	deviation of postimpact 5 year flood from preimpact value (m^3/s).
ΔMFH	monthly flow deviation index (m^3/s/yr).
ΔRBF	mean difference between natural and altered RBF values (1/d).
Δt	operational time interval (= 1 h).
γ	fraction of daily release (for domestic water supply) in period d_1 (−).
η	efficiency of power generation (%).
λ_1, λ_2	environmental flow proportions of the Nanshih and Peishih Creeks (−).

Appendix A: Current Release Rules

A1. Release for Domestic Water Supply

[64] The daily amount of release for the domestic water supply, $\mathrm{DR}^{i,j,k}$, is determined by

$$\mathrm{DR}^{i,j,k} = C_{RC}\left(D^{i,j,k} - 24\Delta t Q_N^{i,j,k,1}\right), \tag{A1}$$

where $D^{i,j,k}$ = projected daily domestic demand on the *k*th day of the *j*th month, *i*th year (Table 1); $Q_N^{i,j,k,1}$ = flow from the Nanshih Creek at the first hour of the *k*th day, *j*th month, *i*th year; Δt = time interval (= 1 h = 3600 s); C_{RC} = release coefficient ranging between [0,1], determined by the reservoir water level and rule curves (Figure 12), expressed as

$$C_{\mathrm{RC}} = \begin{cases} 1, & \text{if } \mathrm{EL}_F^{i,j,k,1} \geq \mathrm{RC}_1^{j,k} \\ 1, & \text{if } \mathrm{RC}_2^{j,k} \leq \mathrm{EL}_F^{i,j,k,1} < \mathrm{RC}_1^{j,k} \\ C_{\mathrm{RC}}^3, & \text{if } \mathrm{RC}_3^{j,k} \leq \mathrm{EL}_F^{i,j,k,1} < \mathrm{RC}_2^{j,k} \\ C_{\mathrm{RC}}^4, & \text{if } \mathrm{RC}_4^{j,k} \leq \mathrm{EL}_F^{i,j,k,1} < \mathrm{RC}_3^{j,k} \\ C_{\mathrm{RC}}^5, & \text{if } \mathrm{EL}_F^{i,j,k,1} < \mathrm{RC}_4^{j,k} \end{cases}, \tag{A2}$$

where $\mathrm{EL}_F^{i,j,k,1}$ = reservoir water level at the 1st hour of the kth day, jth month, ith year; $\mathrm{RC}_1^{j,k}$, $\mathrm{RC}_2^{j,k}$, $\mathrm{RC}_3^{j,k}$, and $\mathrm{RC}_4^{j,k}$ denote the upper, middle, lower, and critical rule curves, respectively, of the kth day, jth month. Currently, $C_{\mathrm{RC}}^3 = 1, C_{\mathrm{RC}}^4 = 0.9$, and $C_{\mathrm{RC}}^5 = 0.7$ are used, which are based on the recommendations made by the Water Resources Agency of Taiwan, implying that an enforced hedging policy is implemented as the reservoir storage is below the lower rule curve [*TFRA*, 2004].

A2. Release for Hydropower Generation

[65] The hourly release rate $R_{\mathrm{HP}}^{i,j,k,l}$ and release duration for the hydropower generation are determined as follows:

$$R_{\mathrm{HP}}^{i,j,k,l} = \begin{cases} Q_{\mathrm{DP}}(\mathrm{EL}_F^{i,j,k,1}) \quad \text{for 24 h}, & \text{if } \mathrm{EL}_F^{i,j,k,1} \geq \mathrm{RC}_1^{j,k} \\ \begin{cases} Q_{\mathrm{DP}}(\mathrm{EL}_F^{i,j,k,1}) & \text{for } 9 \leq l \leq 16 \\ 0 & \text{for } l < 9 \text{ or } l > 16 \end{cases}, & \text{if } \mathrm{RC}_2^{j,k} \leq \mathrm{EL}_F^{i,j,k,1} < \mathrm{RC}_1^{j,k} \\ 0 \quad \text{for 24 h}, & \text{if } \mathrm{EL}_F^{i,j,k,1} < \mathrm{RC}_2^{j,k} \end{cases} \tag{A3}$$

where Q_{DP} is design discharge for power generation, which varies with the reservoir water level and efficiency of power generation, as shown in Table 4, where the values of Q_{DP} are established to optimize the overall performance of power generation facilities (turbines and generator) [*TFRA*, 2004]. The release rules for hydropower generation do not vary with the day of the week (weekdays and weekend) because the surplus power is sold to the TPC as a supplementary source of electricity for the Taipei metropolitan area.

A3. Release for Flood Control

[66] The hourly release rates for the flood control, $R_{\mathrm{FL}}^{i,j,k,l}$, at the antecedent flood, prepeak, and postpeak stages are determined, respectively, as follows:

$$R_{\mathrm{FL}}^{i,j,k,l} = \begin{cases} \alpha_1 Q_I^{i,j,k,l} & \text{for } \mathrm{EL}_F^{i,j,k,l} \geq 167.5 \\ \alpha_2 Q_I^{i,j,k,l} & \text{for } 165 \leq \mathrm{EL}_F^{i,j,k,l} < 167.5 \\ 0 & \text{for } \mathrm{EL}_F^{i,j,k,l} < 165 \end{cases}, \text{ if } T_I \leq Q_I^{i,j,k,l} < 500, \tag{A4a}$$

$$R_{\mathrm{FL}}^{i,j,k,l} = \begin{cases} 500 + \alpha_3\left(Q_I^{i,j,k,l} - 500\right) & \text{for } \mathrm{EL}_F^{i,j,k,l} \geq 167.5 \\ 500 + \alpha_4\left(Q_I^{i,j,k,l} - 500\right) & \text{for } 165 \leq \mathrm{EL}_F^{i,j,k,l} < 167.5 \\ 500 + \alpha_5\left(Q_I^{i,j,k,l} - 500\right) & \text{for } 163 \leq \mathrm{EL}_F^{i,j,k,l} < 165 \\ 0 & \text{for } \mathrm{EL}_F^{i,j,k,l} < 163 \end{cases}, \text{ if } Q_I^{i,j,k,l} \geq 500, \tag{A4b}$$

$$R_{\mathrm{FL}}^{i,j,k,l} = \begin{cases} Q_I^{i,j,k,l} + \alpha_6\left(\mathrm{EL}_F^{i,j,k,l} - 165\right) & \text{for } \mathrm{EL}_F^{i,j,k,l} \geq 165 \\ 0 & \text{for } \mathrm{EL}_F^{i,j,k,l} < 165 \end{cases}, \text{ if } Q_I^{i,j,k,l-2} \geq Q_I^{i,j,k,l-1} \geq Q_I^{i,j,k,l}, \tag{A4c}$$

where T_I = threshold of hourly inflow for triggering the first-stage compelling release, with T_I ranging between [200, 500] m^3/s; α_1, α_2, α_3, α_4, α_5 are coefficients ranging between [0,1]; α_6 = coefficient within the range [50, 200] m^2/s. The currently used values are $T_I = 400$ m^3/s, $\alpha_1 = 0.5$, $\alpha_2 = 0.2$, $\alpha_3 = 0.8$, $\alpha_4 = 0.6$, $\alpha_5 = 0.4$, and $\alpha_6 = 100$ m^2/s [*TFRA*, 2004].

Appendix B: Flow Routing

B1. Reservoir Spill

[67] The hourly reservoir spill, $R_{\mathrm{SP}}^{i,j,k,l}$, is evaluated by

$$R_{\mathrm{SP}}^{i,j,k,l} = \max\left\{Q_I^{i,j,k,l} - R_T^{i,j,k,l} - \frac{S_F^{\max} - S_F^{i,j,k,l}}{\triangle t}, \quad 0\right\} \tag{B1}$$

where $S_F^{\max}$ = reservoir capacity (= 384.7 million m^3); $S_F^{i,j,k,l}$ = hourly reservoir storage, which is obtained by the water balance equation:

$$S_F^{i,j,k,l} = S_F^{i,j,k,l-1} + \left(Q_I^{i,j,k,l-1} - R_T^{i,j,k,l-1} - R_{\mathrm{SP}}^{i,j,k,l-1}\right)\triangle t - E^{i,j,k,l-1}, \tag{B2}$$

where $E^{i,j,k,l-1}$ = hourly evaporation loss, estimated by

$$E^{i,j,k,l-1} = \begin{cases} e^{i,j,k} A^{i,j,k,l-1} \triangle t/12 & \text{for } 7 \leq (l-1) \leq 18 \\ 0 & \text{for } (l-1) < 7 \text{ or } (l-1) > 18 \end{cases}, \tag{B3}$$

where $e^{i,j,k}$ = daily evaporation rate (Table 1), evaporation is assumed to take place during the daytime (6:00 A.M. to 6:00 P.M.); $A^{i,j,k,l-1}$ = hourly reservoir surface area.

B2. Flow Below Diversion Weir

[68] The hourly flow at Reach C (below the diversion weir), $Q_C^{i,j,k,l}$, is evaluated by

$$Q_C^{i,j,k,l} = R_{\mathrm{EF}}^{i,j,k,l} + \lambda_1 Q_N^{i,j,k,1} + \max\left\{Q_B^{i,j,k,l} - Q_{\mathrm{DV}}^{i,j,k,l} - \frac{S_C^{\max} - S_C^{i,j,k,l}}{\triangle t}, 0\right\} \quad \text{(B4)}$$

where $S_C^{\max}$ = capacity of the Chingtan Weir (= 3.9 million m^3); $S_C^{i,j,k,l}$ = hourly weir storage, which is also obtained by the water balance equation:

$$S_C^{i,j,k,l} = S_C^{i,j,k,l-1} + \left(Q_B^{i,j,k,l-1} - Q_{DV}^{i,j,k,l-1} - Q_C^{i,j,k,l-1}\right)\triangle t \quad \text{(B5)}$$

[69] **Acknowledgments.** This research was supported by the National Science Council, Taiwan, with the funding granted to FCW (NSC 96-2628-E002-136-MY3) and JTS (NSC 96-2628-E006-258-MY3). We acknowledge the Taipei Feitsui Reservoir Administration and Taiwan Power Company for the hourly flow and operation data. Reviews provided by two anonymous referees and the Associate Editor help improve the clarity of presentation significantly.

References

Arthington, A. H., S. E. Bunn, N. L. Poff, and R. Naiman (2006), The challenge of providing environmental flow rules to sustain river ecosystems, *Ecol. Appl.*, *16*, 1311–1318.

Baker, D. B., R. P. Richards, T. T. Loftus, and J. K. Kramer (2004), A new flashiness index: Characteristics and applications to midwestern rivers and streams, *J. Am. Water Res. Assoc.*, *40*, 503–522.

Batalla, R. J., C. M. Gómez, and G. M. Kondolf (2004), Reservoir-induced hydrologic changes in the Ebro river basin (NE Spain), *J. Hydrol.*, *290*, 117–136.

Battin, T. J., L. A. Kaplan, J. D. Newbold, and C. M. E. Hansen (2003), Contributions of microbial biofilms to ecosystem processes in stream mesocosms, *Nature*, *426*, 439–442.

Biggs, B. J., and M. E. Close (1989), Periphyton biomass dynamics in gravel bed rivers: The relative effects of flows and nutrients, *Freshwater Biol.*, *22*, 209–231.

Blinn, W., J. P. Shannon, L. E. Stevens, and J. P. Carder (1995), Consequences of fluctuating discharge for lotic communities, *J. N. Am. Benthol. Soc.*, *14*, 233–248.

Boon, P. J. (1993), Distribution, abundance and development of trichoptera larvae in the River North Tyne following the commencement of hydroelectric power generation, *Reg. Rivers Res. Manage.*, *8*, 211–224.

Botter, G., S. Basso, A. Porporato, I. Rodriguez-Iturbe, and A. Rinaldo (2010), Natural streamflow regime alterations: Damming of the Piave river basin (Italy), *Water Resour. Res.*, *46*, W06522, doi:10.1029/2009WR008523.

Bradford, M. J. (1997), An experimental study of stranding of juvenile salmonids on gravel bars and in side channels during rapid flow decreases, *Reg. Rivers Res. Manage.*, *13*, 395–401.

Bratrich, C., B. Truffer, K. Jorde, J. Markard, W. Meier, A. Peter, M. Schneider, and B. Wehrli (2004), Green hydropower: A new assessment procedure for river management, *River Res. Appl.*, *20*, 865–882.

Breil, P., N. B. Grimm, and P. Vervier (2007), *Chapter 6: Surface water-groundwater exchange processes and fluvial ecosystem function: An analysis of temporal and spatial scale dependency, in Hydroecology and Ecohydrology: Past, Present and Future*, edited by Wood, P. J., D. M. Hannah, and J. P. Sadler, John Wiley, Hoboken, N. J.

Bruno, M. C., B. Maiolini, M. Carolli, and L. Silveri (2010), Short time-scale impacts of hydropeaking on benthic invertebrates in an Alpine stream (Trentino, Italy), *Limnologica*, *40*, 281–290.

Céréghino, R., M. Legalle, and P. Lavandier (2004), Drift and benthic population structure of the mayfly Rhithrogena semicolorata (Heptageniidae) under natural and hydropeaking conditions, *Hydrobiologia*, *519*, 127–133.

Cushman, R. M. (1985), Review of ecological effects of rapidly varying flows downstream of hydroelectric facilities, *N. Am. J. Fish. Manage.*, *5*, 330–339.

Dittmann, R., F. Froehlich, R. Pohl, and M. Ostrowski (2009), Optimum multi-objective reservoir operation with emphasis on flood control and ecology, *Nat. Hazards Earth Syst. Sci.*, *9*, 1973–1980.

Freeman, M. C., Z. H. Bowen, K. D. Bovee, and E. R. Irwin (2001), Flow and habitat effects on juvenile fish abundance in natural and altered flow regimes, *Ecol. Appl.*, *11*, 179–190.

Gao, Y., R. M. Vogel, C. N. Kroll, N. L. Poff, and J. D. Olden (2009), Development of representative indicators of hydrologic alteration, *J. Hydrol.*, *374*, 136–147.

Halleraker, J. H., H. Sundt, K. T. Alfredsen, and G. Dangelmaier (2007), Application of multiscale environmental flow methodologies as tools for optimized management of a Norwegian regulated national salmon watercourse, *River Res. Appl.*, *23*, 493–510.

Harman, C., and M. Stewardson (2005), Optimizing dam release rules to meet environmental flow targets, *River Res. Appl.*, *21*, 113–129.

Higgins, A. J., B. A. Bryan, I. C. Overton, K. Holland, R. E. Lester, D. King, M. Nolan, and J. D. Connor (2011), Integrated modelling of cost-effective siting and operation of flow-control infrastructure for river ecosystem conservation, *Water Resour. Res.*, *47*, W05519, doi:10.1029/2010WR009919.

Homa, E., R. M. Vogel, M. P. Smith, C. D. Apse, A. Huber-Lee, and J. Sieber (2005), An optimization approach for balancing human and ecological flow needs, paper presented at EWRI 2005 World Water Environ. Resour. Congress, Anchorage, Alaska, 15–19 May.

Hughes, D. A., and S. J. L. Mallory (2008), Including environmental requirements as part of real-time water resources managements, *River Res. Appl.*, *24*, 852–861.

Korman, J., and S. E. Campana (2009), Effects of hydropeaking on nearshore habitat use and growth of age-0 rainbow trout in a large regulated river, *Trans. Am. Fish. Soc.*, *138*, 76–87.

Magilligan, F. J., K. H. Nislow, and F. J. Graber (2003), A scale-independent assessment of discharge reduction and riparian dis-connectivity following flow regulation by dams, *Geology*, *31*, 569–572.

Magilligan, F. J., and K. H. Nislow (2005), Changes in hydrologic regime by dams, *Geomorphology*, *71*, 61–78.

Mathews, R., and B. D. Richter (2007), Application of the indicators of hydrologic alteration software in environmental flow setting, *J. Am. Water Res. Assoc.*, *43*, 1400–1413.

Meile, T., J. L. Boillat, and A. J. Schleiss (2011), Hydropeaking indicators for characterization of the Upper-Rhone River in Switzerland, *Aquat. Sci.*, *73*, 171–182.

Naiman, R. J., S. E. Bunn, C. Nilsson, G. E. Petts, G. Pinay, and L. C. Thompson (2002), Legitimizing fluvial systems as users of water: An overview, *Environ. Manage.*, *30*, 455–467.

Paetzold, A., C. Yoshimura, and K. Tockner (2008), Riparian arthropod responses to flow regulation and river channelization, *J. Appl. Ecol.*, *45*, 894–903.

Perry, S. A., and W. B. Perry (1986), Effects of experimental flow regulation on invertebrate drift and stranding in the Flathead and Kootenai rivers, Montana, USA, *Hydrobiologia*, *134*, 171–182.

Petts, G. E., J. Nestler, and R. Kennedy (2006), Advancing science for water resources management, *Hydrobiologia*, *565*, 277–288.

Pinay, G., C. Ruffinoni, and A. Fabre (1995), Nitrogen cycling in two riparian forest soils under different geomorphic conditions, *Biogeochemistry*, *30*, 9–29.

Poff, N. L., J. D. Allan, M. B. Bain, J. R. Karr, B. D. Prestegaard, B. D. Richter, R. E. Sparks, and J. C. Stromberg (1997), The natural flow regime: A paradigm for river conservation and restoration, *Bioscience*, *47*, 769–784.

Poff, N. L., J. D. Olden, D. M. Merritt, and D. M. Pepin (2007), Homogenization of regional river dynamics by dams and global biodiversity implications, *Proc. Natl. Acad. Sci. U. S. A.*, *104*, 5732–5737.

Pringle, C. M. (2001), Hydrologic connectivity and the management of biological reserves: A global perspective, *Ecol. Appl.*, *11*, 981–998.

Reichold, L., E. M. Zechman, E. D. Brill, and H. Holmes (2010), Simulation-optimization framework to support sustainable watershed development by mimicking the predevelopment flow regime, *J. Water Res. Plann. Manage.*, *136*, 366–375.

Renöfält, B. M., R. Jansson, and C. Nilsson (2010), Effects of hydropower generation and opportunities for environmental flow management in Swedish riverine ecosystems, *Freshwater Biol.*, *55*, 49–67.

Richter, B. D., J. V. Baumgartner, J. Powell, and D. P. Braun (1996), A method for assessing hydrologic alteration within ecosystems, *Conserv. Biol.*, *10*(4), 1163–1174.

Richter, B. D., J. V. Baumgartner, R. Wigington, and D. P. Braun (1997), How much water does a river need, *Freshwater Biol.*, *37*(1), 231–249.

Richter, B. D., J. V. Baumgartner, D. P. Braun, and J. Powell (1998), A spatial assessment of hydrologic alteration within a river network, *Reg. Rivers Res. Manage.*, *14*, 329–340.

Richter, B. D., and G. A. Thomas (2007), Restoring environmental flows by modifying dam operations, *Ecol. Soc.*, *12*, 12. [Available at: www.ecologyandsociety.org/vol12/iss1/art12/.].

Saltveit, S. J., J. H. Halleraker, J. V. Arnekleiv, and A. Harby (2001), Field experiments on stranding in juvenile Atlantic salmon (Salmo salar) and brown trout (Salmo trutta) during rapid flow decreases caused by hydropeaking, *Reg. Rivers Res. Manage.*, *17*, 609–622.

Sawyer, A. H., M. B. Cardenas, A. Bomar, and M. Mackey (2009), Impact of dam operations on hyporheic exchange in the riparian zone of a regulated river, *Hydrol. Process*, *23*, 2129–2137.

Scruton, D. A., L. M. N. Ollerhead, K. D. Clarke, C. Pennel, K. Alfredsen, A. Harby, and D. Kelley (2003), The behavioral response of juvenile Atlantic salmon (Salmo salar) and brook trout (Salvelinus fontinalis) to experimental hydropeaking on a Newfoundland (Canada) river, *River Res. Appl.*, *19*, 577–587.

Shiau, J.-T., and F.-C. Wu (2004a), Assessment of hydrologic alterations caused by Chi-Chi diversion weir in Chou-Shui Creek, Taiwan: Opportunities for restoring natural flow conditions, *River Res. Appl.*, *20*, 401–412.

Shiau, J.-T., and F.-C. Wu (2004b), Feasible diversion and instream flow release using range of variability approach, *J. Water Res. Plann. Manage.*, *130*, 395–404.

Shiau, J.-T., and F.-C. Wu (2006), Compromise programming methodology for determining instream flow under multiobjective water allocation criteria, *J. Am. Water Res. Assoc.*, *42*, 1179–1191.

Shiau, J.-T., and F.-C. Wu (2007a), A dynamic corridor-searching algorithm to seek time-varying instream flow releases for optimal weir operation: Comparing three indices of overall hydrologic alteration, *River Res. Appl.*, *23*, 35–53.

Shiau, J.-T., and F.-C. Wu (2007b), Pareto-optimal solutions for environmental flow schemes incorporating the intra-annual and interannual variability of the natural flow regime, *Water Resour. Res.*, *43*, W06433, doi:10.1029/2006WR005523.

Shiau, J.-T., and F.-C. Wu (2008), A histogram matching approach for assessment of flow regime alteration: Application to environmental flow optimization, *River Res. Appl.*, *24*, 914–928.

Shiau, J.-T., and F.-C. Wu (2009), Regionalization of natural flow regime: Application to environmental flow optimization at ungauged sites, *River Res. Applic.*, *25*, 1071–1089.

Shiau, J.-T., and F.-C. Wu (2010), A dual active-restrictive approach to incorporating environmental flow targets into existing reservoir operation rules, *Water Resour. Res.*, *46*, W08515, doi:10.1029/2009WR008765.

Singer, M. B. (2007), The influence of major dams on hydrology through the drainage network of the Sacramento River basin, California, *River Res. Appl.*, *23*, 55–72.

Suen, J. P., and J. W. Eheart (2006), Reservoir management to balance ecosystem and human needs: Incorporating the paradigm of the ecological flow regime, *Water Resour. Res.*, *42*, W03417, doi:10.1029/2005WR004314.

Szemis, J. M., H. R. Maier, and G. C. Dandy (2012), A framework for using ant colony optimization to schedule environmental flow management alternatives for rivers, wetlands, and floodplains, *Water Resour. Res.*, *48*, W08502, doi:10.1029/2011WR011276.

Taipei Feitsui Reservoir Administration (TFRA) (2004), *Regulation Rules of the Feitsui Reservoir*, TFRA, Taipei, Taiwan.

van Looy, K., H. Jochems, S. Vanacker, and E. Lommelen (2007), Hydropeaking impact on a riparian ground beetle community, *River Res. Appl.*, *23*, 223–233.

Whiting, P. J. (2002), Streamflow necessary for environmental maintenance, *Annu. Rev. Earth Planet. Sci.*, *30*, 181–206.

Yin, X. A., Z. F. Yang, and G. E. Petts (2011), Reservoir operating rules to sustain environmental flows in regulated rivers, *Water Resour. Res.*, *47*, W08509, doi:10.1029/2010WR009991.

Zimmerman, J. K. H., B. H. Letcher, K. H. Nislow, K. A. Lutz, and F. J. Magilligan (2010), Determining the effects of dams on subdaily variation in river flows at a whole-basin scale, *River Res. Appl.*, *26*, 1246–1260.

Zolezzi, G., A. Bellin, M. C. Bruno, B. Maiolini, and A. Siviglia (2009), Assessing hydrologic alterations at multiple temporal scales: Adige River, Italy, *Water Resour. Res.*, *45*, W12421, doi:10.1029/2008WR007266.